Research Article

Received: 14 March 2023 Revised: 4 May 2023 Accepted article published: 6 May 2023 Published online in Wiley Online Library: 24 May 2023

(wileyonlinelibrary.com) DOI 10.1002/jctb.7419

Analyzing the sustainability of intensified side-stream extractive distillation for binary azeotropic separation: a comparative study

Zong Yang Kong,[a,b] Eduardo Sánchez-Ramírez,[c] Ao Yang,[d,e*] Juan Gabriel Segovia-Hernández[c*] and Jaka Sunarso[f]

Abstract

BACKGROUND: The sustainability performance of extractive distillation (ED) that collectively considers energy efficiency, process safety, economic profitability, process control, and environmental emission has not been widely reported. Motivated by this lack of research, we analyzed and compared the sustainability performance of the intensified side-stream ED (SSED) with that of the conventional extractive distillation (CED) for the separation of binary azeotropic mixtures. Two different design approaches were analyzed; the first approach involves designing the intensified SSED by preserving the original CED column configuration, while the second approach involves optimizing the original column configuration to become a new intensified SSED configuration.

RESULTS: We found that preserving the original configuration usually provides energy-savings, but this advantage is not guaranteed unless the process is optimized. Generally, the reduction in energy consumption improves economic and environmental performance. However, the optimized design has a higher risk index because it is usually larger in size, for the sake of lowering the energy consumption. In addition, the optimized design usually has a higher condition number, which signifies that a more complex control structure is required.

CONCLUSION: Altogether, designing the intensified process *via* process optimization does not always guarantee significant improvement in all sustainability indicators.

Supporting information may be found in the online version of this article.

Keywords: sustainability; extractive distillation; azeotropic separation; process control; process optimization; process intensification

ABBREVIATIONS

AD	Azeotropic distillation
BLEVE	Boiling liquid expanding vapor explosion
CN	Condition number
CED	Conventional extractive distillation
DWC	Dividing wall column
DMF	Dimethylformamide
DMSO	Dimethyl sulfoxide
DETL	Differential Evolution with Tabu List
DDE	Dynamic data exchange
DE	Differential evolution
ED	Extractive distillation
EDWC	Extractive dividing wall column
EDC	Extractive distillation column
EG	Ethylene glycol
EI-99	Eco-Indicator 99
HAZOP	Hazard and operability study
HP	High-pressure
IR	Individual risk
FC	Flow controller
GA	Genetic algorithm

* Correspondence to: A Yang, College of Safety Engineering, Chongqing University of Science & Technology, Chongqing, 401331, P.R. China, E-mail: aoyang2021@cqust.edu.cn; or JG Segovia-Hernández, Universidad de Guanajuato, Campus Guanajuato, División de Ciencias Naturales y Exactas, Departamento de Ingeniería Química, Noria Alta s/n, Guanajuato, 36050, Gto, Mexico. E-mail: gsegovia@ugto.mx

a *Department of Engineering, School of Engineering and Technology, Sunway University, Bandar Sunway, Malaysia*

b *School of Energy and Chemical Engineering, Xiamen University Malaysia, Sepang, Malaysia*

c *División de Ciencias Naturales y Exactas, Departamento de Ingeniería Química, Universidad de Guanajuato, Campus Guanajuato, Guanajuato, Mexico*

d *College of Safety Engineering, Chongqing University of Science & Technology, Chongqing, P.R. China*

e *Chongqing Key Laboratory for Oil and Gas Production Safety and Risk Control, Chongqing, P.R. China*

f *Research Centre for Sustainable Technologies, Faculty of Engineering, Computing and Science, Swinburne University of Technology, Kuching, Malaysia*

LC	Level controller
LP	Low-pressure
MP	Medium-pressure
PI	Process intensification
PSBD	Pressure swing batch distillation
PSD	Pressure swing distillation
PC	Pressure controller
QRA	Quantitative risk analysis
RGA	Relative gain array
RD	Reactive distillation
SI	Sequential iterative
SA	Simulated annealing
SSED	Side-stream extractive distillation
SRC	Solvent recovery column
SVD	Singular value decomposition
TC	Thermally coupled
TAC	Total annual cost
TCED	Thermally coupled extractive distillation
THF	Tetrahydrofuran
TL	Tabu list
UVCE	Unconfined vapor cloud explosion

INTRODUCTION

The products generated through chemical engineering concepts are essential to human well-being, but they also contribute to the degradation of ecosystems that are essential to sustaining all human activities. For the sake of sustainability, chemical engineering must address this paradox by developing chemical products and processes that meet the needs of present and future generations without deteriorating the environment. Efforts toward the design of sustainable chemical processes must consider the role of ecosystems in supporting industrial activities and the effects of human behavior and markets on the environment by their use of chemicals. A close interaction between the fundamentals of chemical engineering and current concepts of sustainability in process systems engineering is needed, along with a change in the engineering paradigm towards generating products with a minimal impact on the environment.

Today, accounting for the sustainability aspects in the early design stage of intensified processes, such as thermally coupled (TC),[1,2] dividing wall column (DWC),[3,4] and side-stream (SS),[5,6] can help distinguish between processes that are easy or difficult to operate.[7] To achieve this, Jiménez-González *et al*. suggested the additional consideration of different 'green metrics', such as environmental, safety, and process control, when designing an intensified process, with aim of achieving a wider goal of environmental sustainability.[8] This is because process intensification (PI) of a given process generally involves topological changes in the process configuration, such as reducing the amount of equipment, which may potentially affect the control properties and performance of the given system.[4] In contrast, reducing the amount of equipment or the column size (e.g., column diameter) usually provides substantial improvements to the economic aspect of the intensified process. Thus, it is necessary to ensure that the column diameter of the intensified process is small to provide these economic benefits while ensuring that the controllability of the process does not deteriorate. On the other hand, the process safety of a given process (e.g., distillation-based process) is highly dependent on the amount of matter inside the system. In the presence of water, for example, a large outflow (e.g., distillate or bottom flowrate) commonly reduces the probability of hazards, which translates to a lower process safety index. Nonetheless, a large outflow will potentially impact the material balance of the system and this can affect the recovery and product purities. Another typical example is the role of the reflux ratio, where a high reflux ratio generally dilutes the internal flow of a system (in the presence of water), thus minimizing the probability of a catastrophic event. Nonetheless, high reflux ratio has a direct impact on the reboiler duty, since increasing the reflux ratio increases the reboiler energy consumption, which eventually affects the economic and environmental impact of a given process. To this end, it is important to account for these different 'green metrics' as an integral part of the process design and operation that has been overlooked in most existing studies on the separation of azeotropic mixtures using extractive distillation (ED).

Based on our literature review, most of the existing studies in ED for the separation of azeotropic mixtures tend to solely prioritize the economic aspects, although some studies in recent years have started to consider environmental, safety, and/or control aspects.[9] On the other hand, sustainability studies that consider the different 'green metrics' in reactive distillation (RD) are much more mature. One such study compares the sustainability performance between TC and DWC for the methyl-ethyl ketone purification process.[4] In addition to the traditional economic aspects, they also considered the 'green metrics', i.e., environmental, safety, and process control, as suggested by Jiménez-González *et al*.[8] Using the same metrics, Amezquita-Ortiz *et al*. examined the sustainability performance of the TC in comparison to Petlyuk for an acetone purification process.[1] A similar study (this one comparing the sustainability of TC and DWC) was also conducted for recovering valuable compounds from wastewater in the nylon industry.[10] The sustainability performances of TC, DWC, and Petyluk in RD for facilitating a sustainable lactic acid purification steady-state process were investigated by González-Navarrete *et al*.[3] Altogether, these studies highlight the role played by these 'green metrics' (according to Jimenez-Gonzalez *et al*.)[8] as crucial characteristics of a sustainable intensified process, in agreement with several other review papers.[11-13] In comparison to the sustainability studies performed for RD, our literature review has indicated that sustainability studies for ED have received limited attention. Motivated by this, the primary objective of this study is to analyze the different 'green metrics' of the intensified ED processes for the separation of binary azeotropic mixtures.

In addition to analyzing the sustainability of the intensified ED, it is interesting to note that process optimization plays an important role during the design of an intensified process to ensure that the process is designed at its optimal conditions. Upon analyzing the 55 recent studies on azeotropic mixture covered in our previous review,[9] we found that more than 70% of the existing studies have attempted to optimize their proposed process using different optimization algorithms, ranging from the traditional sequential iterative (SI) approach to the modernized genetic algorithm (GA) or simulated annealing (SA). Instead of optimizing the intensified process to obtain the optimum configuration, another alternative method is to totally preserve the original column configuration from the existing studies[14-16] for the sake of simplicity. This also eases the comparison process, where the energy-saving efficiency contributed by the PI becomes more apparent relative to the conventional case (i.e., original configuration). Wu *et al*. critically examined the energy-saving efficiency of the extractive DWC (EDWC) used in three industrial cases and designed by preserving the original conventional ED (CED) column configuration.[14] Later, they extended the same design

method (i.e., preserving the original column configuration) to analyze the energy-saving efficiency of the heterogeneous azeotropic distillation system.[15] Recently, we employed the same design method for a preliminary analysis of the economic and environmental performances of different intensified ED for the separation of dichloromethane and methanol.[16] It is worth noting that, in some studies, this method is known as retrofitting or revamping, and it can involve, for example, adding trays to the existing column or replacing the condenser(s) or reboiler(s).[17] To our knowledge, however, these changes are not widely employed by the existing studies in the field of ED[14,15] for the reasons explained earlier. To date, there are no existing studies analyzing the difference between optimizing and preserving the original column configuration when designing an intensified process for azeotropic separation using ED. Here, it is worth highlighting that optimizing the column configurations of the intensified process does not necessarily lead to savings in energy or TAC, as revealed by several existing studies.[18-21] Therefore, the performance of the different sustainability metrics under these two approaches is not clear at this stage. Thus, another contribution (i.e., secondary contribution) of this work is to explore which design approach (i.e., preserving the original column configuration or optimizing the new intensified SSED configuration) provides a better sustainability performance.

In summary, we analyze the sustainability performance of the different intensified SSED configurations for the separation of azeotropic mixtures based on their energy, economic, environmental, process safety, and process control. Here, it is not our intention to link PI with new process synthesis, optimization algorithm, or conventional PI process control, but we do analyze all the sustainability metrics of the intensified SSED under two different design approaches (i.e., the first approach involves preserving the original column configuration from the existing study, while the second approach involves optimizing the original column configuration so that it becomes a new SSED configuration). During the optimization process, we first considered only the economic indicator as our primary objective function to initially identify which sustainability indicators play a greater role and ensure that these indicators can be considered for multi-objective optimization in future work. Two different case studies were used in this study and their detailed descriptions are available in the Case Studies Description section. The methodology involved in this study is elaborated in the Methodology section, while the details of the different 'green metrics' are explained in the Sustainability Evaluation section. The Results and Discussion section provides the result analysis and discussion, while the Conclusions section concludes this work by summarizing the important findings.

DESCRIPTION OF CASE STUDIES

Case study 1

The first case study is based on the binary azeotropic mixture of dichloromethane and methanol, which is commonly obtained from the discharge of prednisolone manufacturing.[22,23] This binary mixture could be harmful to human health and the environment[24-26] and, thus, proper separation and resource recovery is essential to facilitating environmental protection. Nonetheless, a minimum boiling azeotrope is formed when the methanol purity is 13.87 mol% at atmospheric pressure, implying that these two components are unable to be effectively separated using normal distillation techniques and, thus, require the use of advanced distillation. Today, our literature review found three existing studies that worked on the separation of dichloromethane and methanol.[16,23,27] Among these three studies, the most recent one[16] explored the possibility of further enhancing the economic and environmental performances of ED from the previous work[27] by using different PI techniques, such as side-stream extractive distillation (SSED), thermally coupled extractive distillation (TCED), and EDWC. Here, it is worth highlighting that all the intensified processes (e.g., SSED, TCED, and EDWC) in the previous study were designed by preserving the original CED column configuration. In this work, we introduced an optimized configuration for the corresponding intensified process and compared its sustainability performance against that of the intensified process from previous work.[16] Here, only the SSED is considered because the previous study[16] concludes that the SSED provided the best compromise performance, in terms of economic, environmental, and control metrics, for separating the dichloromethane and methanol. Since the objective of this work is to analyze how sustainability performance differs between optimized and preserved original column designs, we use the preserved original column design that is readily available from our previous work,[16] while the optimized configuration is introduced in this work. The details of the optimization procedure are made available in the Inventory Control section.

Figure 1 shows the CED process configuration reproduced from the previous study.[16] Here, the fresh feed stream containing 17 mol% of methanol and 83 mol% of dichloromethane is fed onto the first column, commonly known as the extractive distillation column (EDC), with the dimethylformamide (DMF) solvent. In the distillate (D1) of EDC, the high purity dichloromethane of at least 99.9 mol% is obtained, while the remainder mixtures are passed onto the solvent recovery column (SRC) for further separation. The high purity methanol of at least 99.9 mol% is obtained from the distillate (D2) of the SRC. Lastly, the recovered DMF obtained from the SRC bottom (B2) is sent to a cooler to lower the temperature before it is subsequently reused in the EDC. A top-up (i.e., make-up) flowrate is introduced to reimburse the solvent lost during the separation processes. The same thermodynamic properties package, non-random two-liquid model (NRTL), was used in this study as in the previous work.[16] However, it is important to note that the accuracy of the thermodynamic properties was not evaluated in this study, as it had already been verified in the previous study.

Case study 2

The second case study is based on the separation of tetrahydrofuran (THF) and ethanol, which form a minimum boiling azeotropic mixture. THF is an important organic solvent that is usually used as a raw material in chemical industries, such as for the manufacturing of adipic acid. Ethanol, on the other hand, is frequently used in pharmaceutical industries for manufacturing drugs and medicines.[28,29] Following this production, it is important to recover these two valuable compounds to promote resource conservation and environmental protection. Currently, our literature search has identified increasing numbers of studies that worked on the recovery of THF and ethanol from binary or ternary azeotropic mixtures in the last 7 years.[18,29-40]

Figure 2 displays the process flow diagram for the separation of THF and ethanol using DMSO reproduced from the most recent study.[41] Aside from the difference in fresh feed mixtures, the process configuration for this case (Fig. 2) is identical to that of case study 1 (Fig. 1) and, therefore, is not explained here again. The thermodynamic properties package utilized for this case is

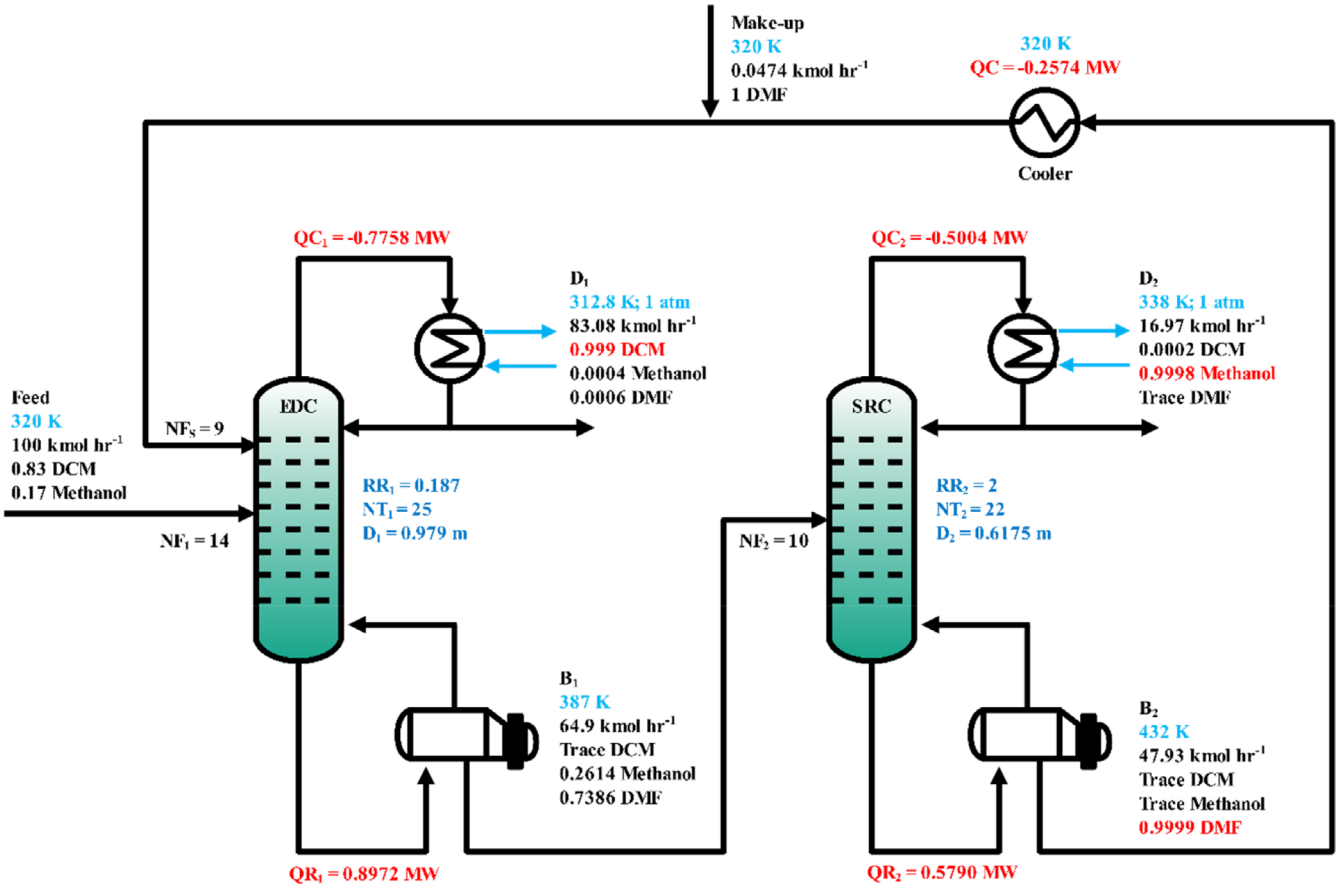

Figure 1. CED reproduced from previous work for the separation of dichloromethane and methanol.[16]

UNIQUAC, which is consistent with the prior research studies.[18,29-40] It is worth noting that this study does not delve into the accuracy of the thermodynamic properties, as this had already been verified in the preceding studies.

METHODOLOGY

Steady-state simulation

The steady-state processes in this work were simulated using Aspen Plus V11. For each case study, two different intensified SSED configurations were simulated. The first configuration was designed by preserving the column configuration of the original base case (i.e., CED) and, thus, all design parameters (e.g., feed and solvent flowrate) were kept the same as those in the previous work. Such methodology was reported to provide a fair economic comparison because any saving benefits from the energy reduction is directly reflected in the TAC. The second configuration involves process optimization, where an optimized column configuration was introduced. Here, the initial values used for process optimization in the second configuration are taken from the first configuration (i.e., preserving original column design).

Preserved original column design

As indicated in the previous section, the first SSED configuration was developed through preserving the original column configuration. This means that the total number of stages, the feed, and the solvent stage location for both EDC and SRC remained unchanged, while other design variables (such as reboiler duty, reflux ratio, distillate rate, side-stream location, and side-stream flowrate) were manipulated manually to meet the minimum product purities. Here, it is important to reiterate that such simulation methodology that preserves the original column configuration has already been employed by existing studies.[14,15] Although it may seem unreasonable to perform such changes because the column configuration changed from CED to SSED and may no longer be at its optimum, it is equally important to note that some studies have reported that optimizing the column configuration does not necessarily guarantee energy savings, as reported by existing studies.[18,19] In practice, retrofitting can still involve changing some of the design parameters, such as feed and solvent stage location and total stage number, as demonstrated by Premkumar and Rangaiah.[17] Generally, minor modifications with small investments are preferred by the industry, especially by those with an investment payback period of less than 3 years. In this work, we attempted to preserve the original column configuration for the purpose of simulation, while ensuring that all the product purities met their desired specifications.

For case 1, the preserved original column configuration was reproduced directly from previous work,[16] while the optimized configuration was developed in this work. On the other hand, both configurations for case 2 were developed in this work.

Optimized design

To run an industry that can successfully compete in the global market, processes must run at their best. The optimization algorithm was developed for each configuration considering their

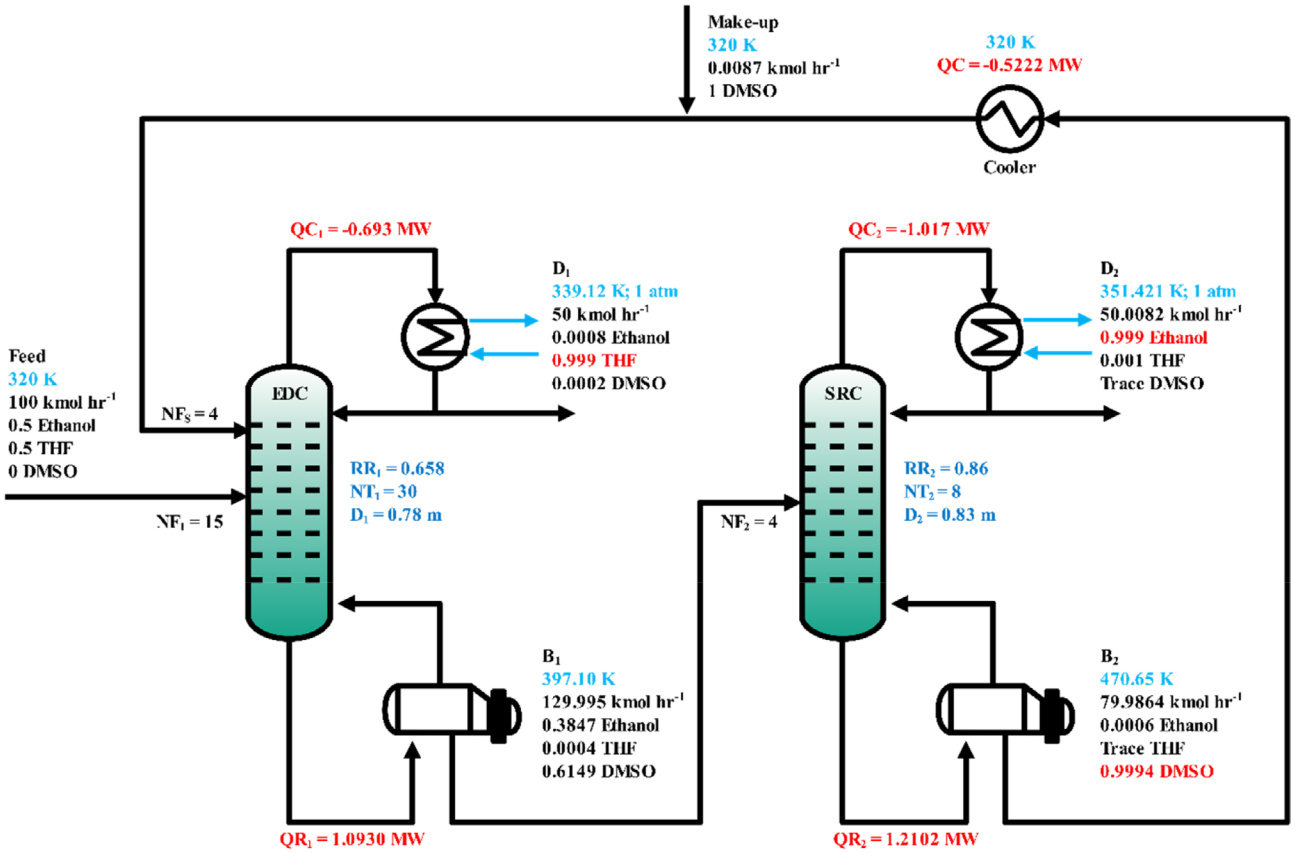

Figure 2. CED using DMSO for the separation of THF and ethanol.

objectives, limitations, and design parameters. All the configurations are conceptualized as limited global optimization problems. The goal of process designs for case 1 and case 2 is to minimize TAC, which is directly associated to energy, operational, and capital costs. This objective is dependent on the needed recoveries and purities in each product stream, as defined by Eqn. (1).

$$\begin{aligned} &\text{Min}\,(\text{TAC}) = f(N_{tn}, N_{fn}, R_{rn}, F_{rn}, D_{cn}) \\ &\text{Subject to}\ \vec{y}_m \geq \vec{x}_m \end{aligned} \tag{1}$$

where N_{tn} is total column stages, N_{fn} is the feed stage in column, R_{rn} is the reflux ratio, F_{rn} is the distillate fluxes, D_{cn} is the column diameter, and y_m and x_m are vectors of the obtained and required purities for the m components, respectively. For each route procedure, this minimization entails the manipulation of 10 continuous and discrete variables, of which 5 are employed for the design of each column. The recoveries of the essential components in each product stream must be considered as a restriction for the optimization problem since the product stream flows are altered.

Specifically, the optimization and design of process routes are highly non-linear and multivariable problems, with both continuous and discontinuous design variables present. Additionally, the objective functions employed as optimization criteria are possibly non-convex, with the potential presence of local optimums and susceptibility to restrictions. Therefore, we applied the stochastic optimization algorithm Differential Evolution with Tabu List (DETL) to the process pathways.[42] GA and differential evolution (DE) are both based on Darwin's theory of natural selection, with one key distinction: while DE encodes decision variables as floating-point numbers, some GA, especially the earlier versions, do so as bit strings. Srinivas and Rangaiah[42] have shown how the DE algorithm can perform better when some metaheuristic tabu notions are included. The tabu list (TL), in particular, can be utilized to reduce revisiting the search space by keeping track of recently visited points and preventing needless function evaluations. This fact led Srinivas and Rangaiah to propose the hybrid method DETL, which combines traditional DE steps with TL and tabu checks to keep track of the evaluated points and prevent returning to them during the optimization search and a convergence criterion based on the maximum number of generations.[42] Srinivas and Rangaiah have provided a thorough explanation of this DETL algorithm.

This optimization strategy was implemented on a hybrid platform using Aspen Plus and Microsoft Excel. Using the dynamic data exchange (DDE), COM technology was employed to send the vector of choice variables (i.e., the design variables) from Aspen Plus to Microsoft Excel. These values are linked in Microsoft Excel to the process variables required by Aspen Plus. After the simulation is complete, Aspen Plus returns the output vector to Microsoft Excel. Microsoft Excel then evaluates the objective function values and suggests new values for the choice variables in accordance with the stochastic optimization technique employed. We used the following DETL technique settings for the process route optimization examined in this study: 120 individuals, 300 generations, 50% of the total population on the tabu list, and, for the crossover, mutation fractions, and tabu radiuses of 0.6, 0.8, and 0.0000025, respectively. Optimization parameters

were considered according to what has been previously reported in the literature.[43-45]

Dynamic simulation

Once the configurations for both cases were obtained, we explored their control (i.e., dynamic) performance and compared them against the base case (i.e., CED). Prior to the dynamic simulation in Aspen Plus Dynamic, all the process equipment was sized accordingly. In this work, the hold-up time and liquid level for the distillation column bottom and condenser drum were 10 min and 50%, respectively. The diameter of the distillation column and its corresponding pressure drop were evaluated automatically using the column internal feature in Aspen Plus. Once all the equipment was sized accordingly and the process simulation was converted into Aspen Plus Dynamic, the inventory and quality control loops can be installed; the details for this are available in the next section.

Inventory control

Figure 3 shows the flowsheet of a SSED configuration equipped with basic inventory control, including level controller (LC), pressure controller (PC), and flow controller (FC). It is worth noting that the inventory control for the CED is analogous to that of the SSED in Fig. 3, except for the fact that the SSED requires an additional FC, as indicated in red (Fig. 3), to maintain the material balance of the overall system.

In Fig. 3, the bases of the EDC and SRC are controlled by manipulating the bottom flowrate. Likewise, the levels of reflux drum for both columns are maintained by using the distillate rate. The fresh feed is flow controlled, while the solvent flowrate is manipulated by the solvent make-up flowrate. A ratio control was additionally installed to maintain the solvent to total fresh feed ratio. These controls applied to both CED and SSED and are commonly found in existing studies.[16,41,46] As indicated previously, an additional FC is present in SSED and a ratio control was employed to maintain the ratio of fresh feed flowrate and side-stream flowrate, for the sake of overall material balance in system.

Quality control

The quality control loop is usually installed after the inventory control has been established. In this work, we only consider the temperature control for tightening the product qualities instead of the composition controllers due to their cost efficiency and operational maintenance difficulty.[47] The open-loop sensitivity analysis, which has been widely employed by existing works,[48,49] was used to determine the temperature-sensitive location (i.e., tray) by incorporating a small change (±0.01%) to the control degree of freedom (e.g., reboiler duty or reflux ratio). The tray location(s) that displayed the largest temperature oscillation (ΔT) was chosen as the temperature-sensitive tray. Luyben described the exhaustive steps of the open-loop sensitivity analysis in his textbook.[50] When the column has two or more temperature-sensitive locations, the best control pairing is determined *via* relative gain array (RGA) analysis.

SUSTAINABILITY EVALUATION

Instead of analyzing the performance of the different SSED configurations in both cases based on economic aspects only, as in most

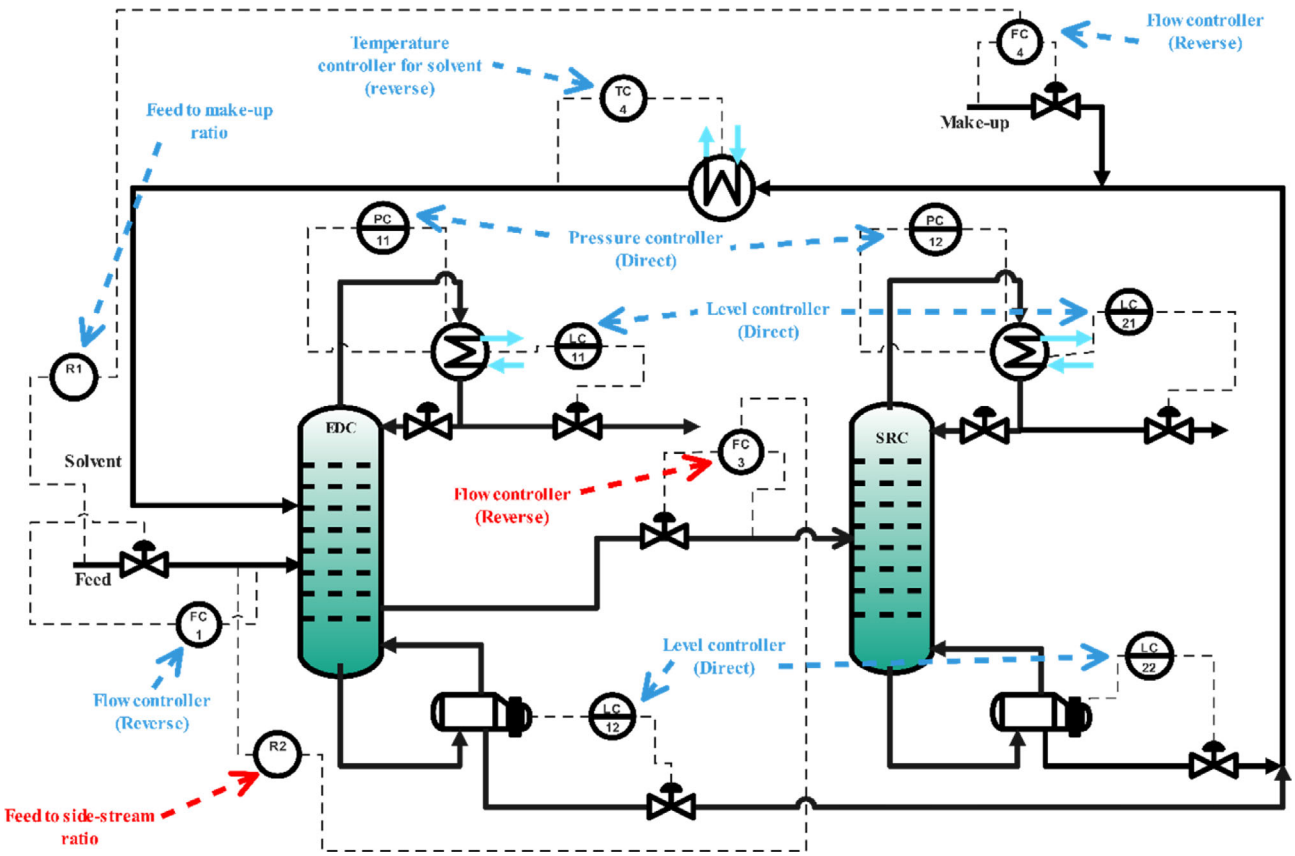

Figure 3. Inventory control loop for the SSED.

of the existing studies, we additionally consider the 'green indicators' (e.g., safety, environmental, and operational controllability) proposed by Jiménez-González *et al.*[8] and Jiménez-González and Constable[13] introduced in the Introduction section.

Economic

The economic index is examined on the basis of TAC,[51] which is calculated *via* Eqn. (2).

$$TAC = \frac{\sum_{i=1}^{n} C_{TM,i}}{n} + \sum_{j=1}^{n} C_{ut,j} \quad (2)$$

where C_{TM} is the capital cost of the plant, n is the total number of individual units, and C_{ut} is the cost of services.

The total module cost is calculated from Eqn. (3).

$$C_{TM} = 1.18 \sum_{i=1}^{n} C^{0}_{BM,i} \quad (3)$$

where the term C^{0}_{BM} represents the cost of the bare module, which reflects the direct and indirect costs for each unit. The term 1.18 depends on the type of chemical plant. If it is a plant that processes fluids, it is the indicated value. This term is calculated by Eqn. (4).

$$C^{0}_{BM} = C_p F^{0}_{BM} \quad (4)$$

In most cases, the bare module cost factor, F^{0}_{BM}, is calculated by Eqn. (5).

$$F^{0}_{BM} = (B_1 + B_2 F_M F_P) \quad (5)$$

The constants, B_1 and B_2, for the bare modulus factor depend on the type of equipment and its description, e.g., pumps, vessels, and heat exchangers. For vertical vessels, B_1 is 2.25 and B_2 is 1.82, while for horizontal vessels, B_1 is 1.49 and B_2 is 1.52.

The pressure factor, F_p, is obtained from Eqn. (6).

$$\log_{10} F_p = C_1 + C_2 \log_{10} P + C_3 (\log_{10} P)^2 \quad (6)$$

For pressures below 5 bar, $C_1 = C_2 = C_3 = 0$. Note that the pressure factors are always greater than 1. The recovery period for the process operating 8500 h per year was set at 10 years. The utilities cost for the high-pressure (HP) (42 bar, 254 °C), medium-pressure (MP) (11 bar, 184 °C), and low-pressure (LP) (6 bar, 160 °C) are \$9.88 GJ^{-1}, \$8.22 GJ^{-1}, \$7.78 GJ^{-1}, respectively, while the cost of cooling water is \$0.72 GJ^{-1}.[52]

Inherent safety

The inherent safety of the proposed process was determined *via* the probability of affectation (i.e., an explicit hazard that occurs in one particular incident), given by Eqn. (7).

$$IR = \sum f_i P_{x,y} \quad (7)$$

The f_i and $P_{x,y}$ in Eqn. (7) are the incident rate and likelihood of a specific hazard resulting from the incident *i*, respectively. The IR is usually estimated via quantitative risk analysis (QRA), where hazards and accidents are identified, along with their resulting consequences. Here, possible scenarios, such as the continuous and instantaneous discharge (i.e., release) from the separation column, are first identified through the hazard and operability study (HAZOP). A continuous leaking (i.e., release) is usually caused by a full or partial pipeline rupture on a process unit that could result in flash fire, jet fire, and toxic release. In contrast, instantaneous discharge is the total loss of the process equipment resulting from a catastrophic rupture, and this may result in boiling liquid expanding vapor explosion (BLEVE), unconfined vapor cloud explosion (UVCE), flash fire, and toxic release. The incidence rate for each individual risk (f_i) can be extracted from a previous report.[53] In this work, an irreversible injury, such as death, is used in the risk assessment due to the widely available data. Once the possible hazards have been identified, it is necessary to carry out the consequence assessment to analyze their probability (i.e., likelihood) $P_{x,y}$ and their associated damages; this includes calculating the physical variables, such as thermal radiation, overpressure, and leakage molarity resulting from the incidents hazard. These variables were also determined using the equations made available by the previous report.[53] The detailed calculations of the IR are given in Appendix A (Supporting Information).

Environmental index

The environmental aspect of the proposed process was examined *via* the Eco-Indicator 99 (EI99), which was initially derived from the life cycle assessment.[54] The EI99 measures the environmental impact initiated by the activities carried out in the process. Today, the EI99 is widely used by different researchers globally to quantify the complete environmental performance of a given chemical processes and promote sustainable design.[4,55] It considers 11 impact categories that belong to three major damages, involving human health, ecosystem quality, and resource depletion, and is given by Eqn. (8).

$$EI99 = \sum_{b} \sum_{d} \sum_{k \epsilon K} \delta_d \omega_d \beta_b \alpha_{b,k} \quad (8)$$

In Eqn. (8), the total amount of chemical *b* released over a flow reference caused by the direct emission is given as β_b, the damage caused in category *k* per unit of chemical *b* discharged to the flora and fauna is given as $\alpha_{b,k}$, the weighting and normalization for the damage in category *d* are given as ω_d and δ_d, respectively. The basis of EI99 in this work is based on 1 point being equivalent to the annual environmental load of one out of one thousand average European residents. There are three main aspects in the impact assessment, including the steam as a heating utility for the reboiler, the electricity needed for pumping, and the construction material (i.e., steel) for the process unit; the parameters employed for the calculations are given in Supporting Information, Table S1. Then, the EI99 in this work employed the hierarchical perspective, which is commonly used by existing distillation studies.[1,3,4,10]

Control properties index

The control performances of the different configurations for both cases were evaluated based on both the theoretical control performance and the dynamic simulation to ensure that both methods provided consistent results. In this sub-section, we describe the theoretical control analysis, while the dynamic simulation has been detailed in the Dynamic Simulation section. The singular value decomposition (SVD) can be employed to examine

the theoretical control performance of the process, as given by Eqn. (9).

$$W = G\alpha V^{H} \tag{9}$$

In Eqn. (9), all the variables are in a matrix, where W represents the target for SVD, G contains the left-singular vector of V, α contains the singular values of V, and H is the left-singular vectors of V. The detailed derivation and explanation of SVD is available in the existing work.[56]

Here, the minimum (σ_{min}) and maximum singular (σ^{max}) values are the two most important parameters. The magnitude (i.e., values) can be obtained *via* MATLAB by simply incorporating the temperature change from open-loop sensitivity analysis, as explained in the Dynamic Simulation section. The condition number (CN) is then calculated based on the proportion of the minimum and maximum singular value, given by Eqn. (10).

$$CN = \frac{\sigma^{max}}{\sigma_{min}} \tag{10}$$

The CN reflects system stability when subjected to different process parameter uncertainties or modelling errors. From Eqn. (10), the process with a lower CN generally translates to a better control performance.[56,57] The CN has been widely employed by several existing studies as an indicator for evaluating the control

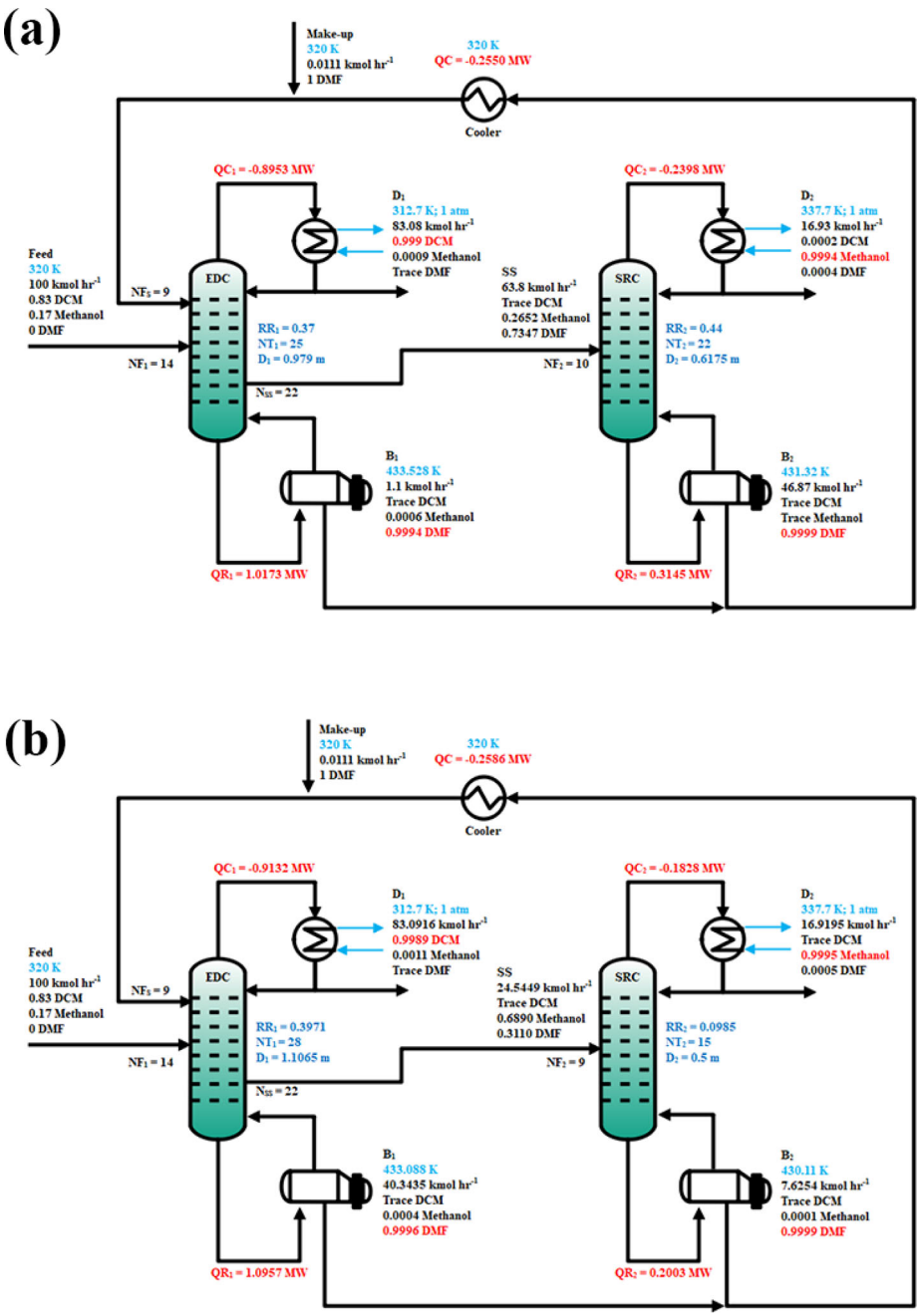

Figure 4. Process flowsheet for the SSED designed by (a) preserving the original column configuration and (b) optimizing the configuration for case 1.

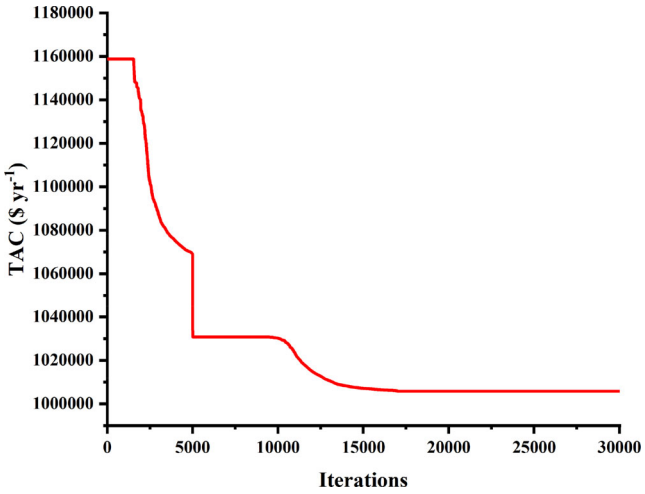

Figure 5. Optimization results of case 1.

performance for different chemical processes.[1,58] It is also often used as one of the objective functions for the multi-objective optimization of different distillation-based processes.[59,60]

RESULTS AND DISCUSSION

Steady-state performance

Case study 1

The process flowsheet for the SSED designed by preserving the original column configuration and process optimization is displayed in Fig. 4, with the optimization results given by Fig. 5. The optimization duration was 55 h. The results comparison of both flowsheets in Fig. 4 against the base case (Fig. 1) is summarized in Table 1.

From Table 1, it is observed that designing the SSED by preserving the original CED column configuration resulted into 10% energy savings, even when the intensified process has not been optimized. Further optimizing the SSED using DETL algorithm provides an additional 3% savings in energy consumption and, altogether, the energy consumption of the optimized configuration is 12% lower than that of the CED. These reductions in energy consumption provide a direct benefit to the economics of the processes, where the TAC values of the preserved and optimized configurations decreased by about 1% and 3%, respectively. Several observations can be made upon meticulous analysis of both intensified processes (Fig. 4) against the base case (Fig. 1). The first observation was that the reboiler temperature of the EDC in both intensified processes (Fig. 4) increased from 387 K to about 433 K, which requires the usage of MP steam, instead of the LP steam used in the CED. This means that the unit price of steam as a heating utility will increase by about 5%, from \$ 7.78 GJ^{-1} to \$ 8.22 GJ^{-1}. This increase, however, was traded-off by the decrease in the total energy consumption, as explained earlier; this decrease is much larger than the increase in the steam unit price and, therefore, there is a net reduction in the TOC, which results in a decrease in TAC. In the optimized configuration (Fig. 4(b)), there is a significant topological change in the process configuration, where the total stage number in the EDC increases from 25 stages to 28 stages, while the total stage number in the SRC decreases from 22 to 15. There was a change in the new feed location for SRC, while the fresh feed and solvent locations in the EDC remained unchanged.

From an environmental perspective, both intensified processes provide reasonable improvements, as evident by the decrease in the EI99 of about 10%. Such a reduction, in our opinion, can mainly be attributed to the decrease in energy consumption. This is because the EI99 is strongly correlated with the energy and steam consumption, which are two of the main factors present in the EI99 calculations, as indicated in the Environmental Index section.

From Table 1, it was found that the IR for all three cases is identical. The IR for the optimized configuration was calculated to be the highest, marginally, and this was mainly attributed to increase in the toxic discharge incident. Here, the toxic discharge incident is highly dependent on the mass of continuous and instantaneous release, which is affected by the flowrate at the condenser and reboiler and by the size of the main column [Supporting Information, Eqns. (S5) and (S6)]. Since there is an overall increase in the column size for the optimized configuration, the IR also increases. For the same reason, the IR for the preserved configuration is lower than that of the base case. Note that the mass of continuous release in the reboiler of the preserved configuration is smaller than that of the base case due to the presence of a side-stream to divert a portion of the material from EDC to SRC, instead of this material flowing through the column bottom, as it does in the base case. This observation agrees with an existing study with similar findings.[61] To further reduce the IR, several existing studies have recommended using less equipment, like in the DWC, to reduce the probability of catastrophic events.[4,55]

As for the control properties, the CN of both intensified processes increases, which generally signifies a worsened controllability for the intensified processes, meaning that a more complex control structure is required. This is expected for the preserved configuration because it has been well reported that the column configuration is strongly linked to an exact composition mixture that affects the control properties of a process. Since the preserved configuration was designed by preserving the CED configuration from previous work, the additional side-stream

Table 1. Result comparison between the preserved and optimized configurations against base case for case 1

		SSED	
Indicators	CED	Preserved configuration	Optimized
Energy (kW)	1476.25	1331.73 (−10%)	1296.02 (−12%)
TAC (\$ Million)	1.070971	1.055775 (−1%)	1.037153 (−3%)
EI99 (Million)	0.270348302	0.242353294 (−10%)	0.242353295 (−10%)
IR (10^{-3})	1.694716	1.694707 (−0.001%)	1.694724 (+0.0005%)
CN	30.33	45.61 (+50%)	57.59 (+90%)

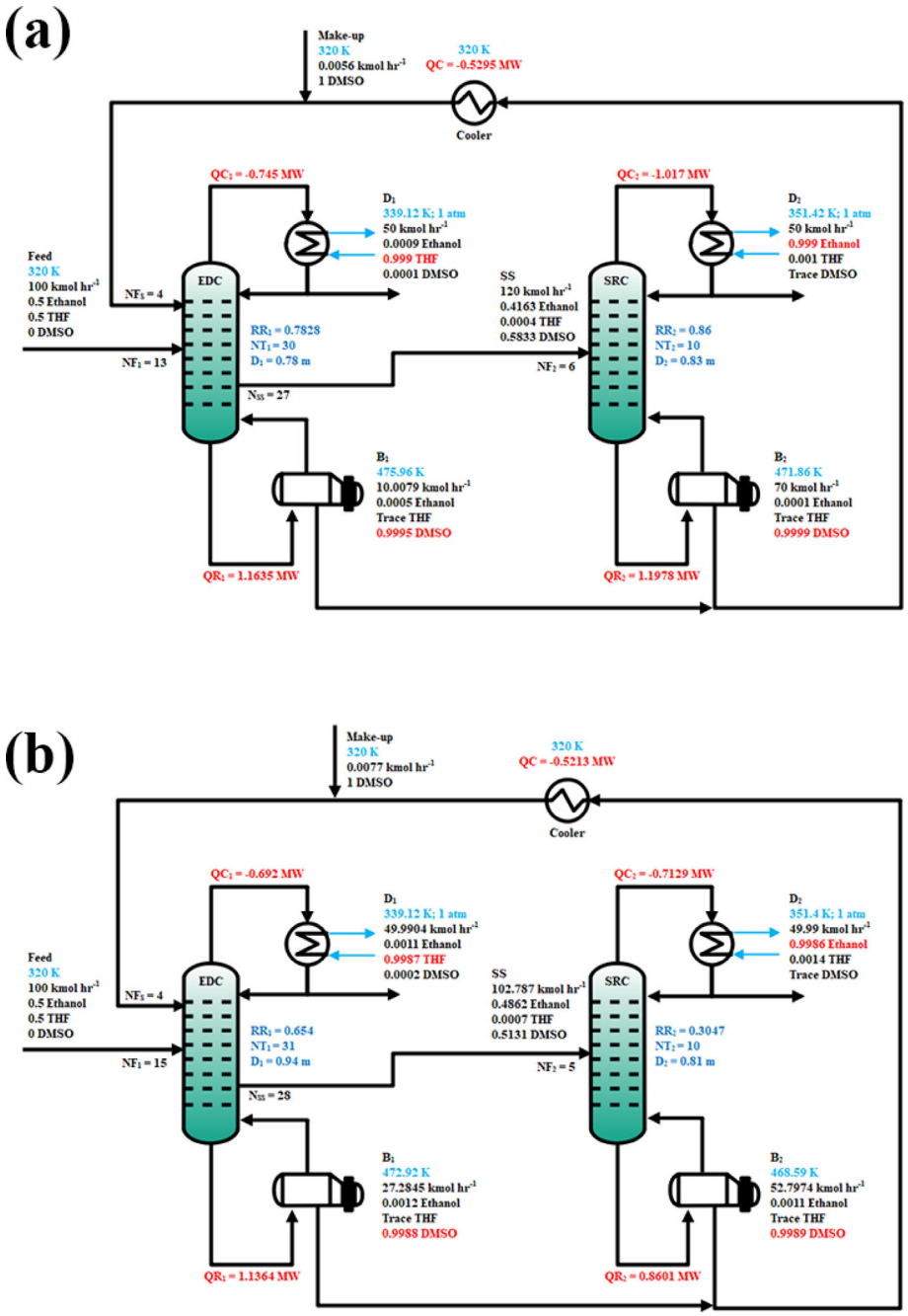

Figure 6. Process flowsheet for the SSED designed by (a) preserving the original column configuration and (b) optimizing the configuration for case 2.

connection will result in slight changes in the composition and stream flow that may potentially affect the controllability of the process.[61] Thus, it is not certain that the theoretical control performance remains analogous due to the non-optimal column configuration. As for the optimized configuration, the surge in the CN is in contrast with several existing studies in literature;[2,62,63] this is still reasonable, in our opinion, because the optimization objective in this work is to minimize TAC without the consideration of theoretical control properties. Hence, it is expected for the optimum design to have the lowest TAC (i.e., best economic process), although it may not necessarily demonstrate the best operational controllability, unless multi-objective optimization is carried out based on economical and theoretical control properties. Note that the previous studies[2,62,63] showing that optimization generally improves the CN, as indicated earlier, are those that involve bi-objective optimization considering economical and theoretical control properties. In this work, since our objective was to preliminarily analyze the effects of designing an intensified process either by maintaining the original system design or by a complete process optimization on the different sustainability indicators, we did not consider multi-objective optimization in this work. To reiterate, here we conduct a preliminary identification of which sustainability indicators play a greater role so that these indicators can be considered for multi-objective optimization in future work.

Overall, both intensified SSED (Fig. 4) processes provided meaningful improvements to most of the green metrics in comparison

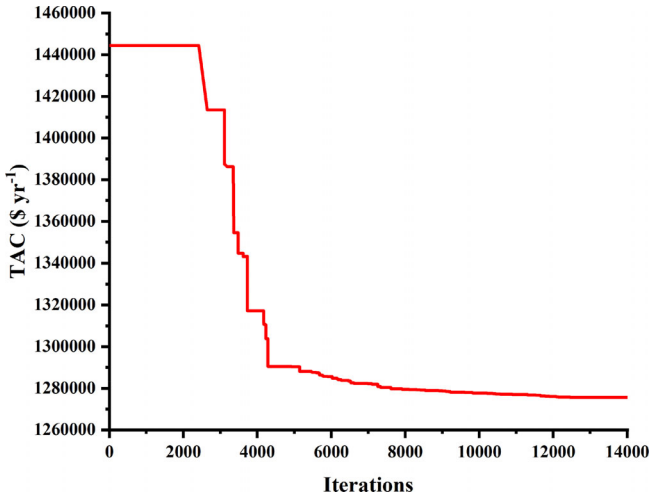

Figure 7. Optimization results of case 2.

to the base case (Fig. 1), highlighting the superiority of the intensified configurations. Among the two intensified configurations, it was found that the optimized configuration provided the lowest energy and TAC, making it the most economic choice. The environmental and safety aspects of the optimized configuration, on the other hand, are inferior to those of the preserved configuration design due to the increase in column size. Lastly, the theoretical control performance of the optimized configuration provided the largest deterioration since it was optimized based only on an economic objective.

Case study 2

The process flowsheet for the SSED designed by preserving the original column configuration and process optimization are displayed in Fig. 6, while the optimization results are given by Fig. 7. The optimization duration was 68.5 h. The results comparison between both flowsheets in Fig. 6 against the base case (Fig. 2) is summarized in Table 2.

From Table 2, it is observed that the SSED designed by preserving the original CED column configuration did not provide any energy savings in comparison to CED, contrary to case 1. Here, the total energy consumption of the preserved configuration increases by about 10% relative to the base case. Optimizing the intensified process in the present case using the same DETL algorithm resulted in significant energy savings of about 13% with respect to the CED, and this facilitated the TAC reduction by about 11%. Analogous to case 1, Fig. 6 shows a significant increase in the reboiler temperature of EDC in both intensified processes from 397 K to about 473 K. This means that the EDC of both intensified processes will require HP steam as heating utility, instead of the LP steam used in the base case. Such an upgrade in heating utility will result in an increase in the steam unit price of about 27% from $7.78 per GJ to $9.88 per GJ, similar to case 1. Nonetheless, this increase was traded-off by the decrease in the total energy consumption (as explained earlier), which is much greater than the increase in the steam unit price and, thus, there is an overall decrease in the TOC that subsequently reduces the TAC. Other than the reboiler temperature, the optimized configuration (Fig. 6(b)) also experienced a marginal change in the topological configuration after optimization, where the total number of stages in EDC increased by 1 stage. There was a change in the new feed location for both EDC and SRC, while the feed locations for solvent in the EDC remained analogous to the base case. These observations are similar to those observed in case 1. In the case of the preserved configuration, the cumulative increases in the energy consumption and steam unit price from LP to HP resulted in an inevitable increase in the TAC of about 16%.

As for the environmental perspective of both intensified processes, one interesting observation from Table 2 is that the preserved configuration does not provide any improvement in the EI99, which contradicts the findings from case 1. One obvious reason for this is that the preserved configuration does not provide any energy savings with respect to the base case; since the energy and steam consumption are two important factors in the EI99 calculations (as indicated in the Environmental Index section), there is a very low possibility that the environmental performance will improve when there is no improvement in energy consumption. For the same reason, the improvement in environmental aspects for the optimized configuration was due to the significant savings in energy consumption by almost the same magnitude, albeit to a slightly lower extent.

The trend of the IR for case 2 is analogous to that observed in case 1, where the IR of the optimized configuration was found to be the highest and that of the preserved configuration was found to be lower than the base case. For the same reason as explained in case 1, these were mainly caused by toxic release incidents, which are highly reliant on the mass of continuous and instantaneous release. The mass of continuous and instantaneous discharges, on the other hand, is dependent on the flowrate at the condenser and reboiler, and on the size of main column, as reflected by the Supporting Information [Eqns. (S5) and (S6)]. In the present case, the column size of the optimized configuration increased, which increased the IR. In case 2, the mass of continuous release in the reboiler of the preserved configuration was marginally lower than that of the base case due to the presence of a side-stream to channel a portion of material from EDC to SRC, which reduced the column bottom flow. This observation is consistent with case 1 and a previous study.[61]

Table 2. Result comparison between the preserved and optimized configurations against base case for case 2

		SSED	
Indicators	CED	Preserved configuration	Optimized
Energy (kW)	2303.17	2545.92 (+10.5%)	1996,46 (−13%)
TAC ($ Million)	1.433898	1.663575 (+16%)	1.276291 (−11%)
EI99 (Million)	0.419	0.459 (+10%)	0.36 (−14%)
IR (10^{-3})	1.686855	1.686852 (−0.0002%)	1.686878 (0.0014%)
CN	569.75	2910.2 (+411%)	4139 (+626%)

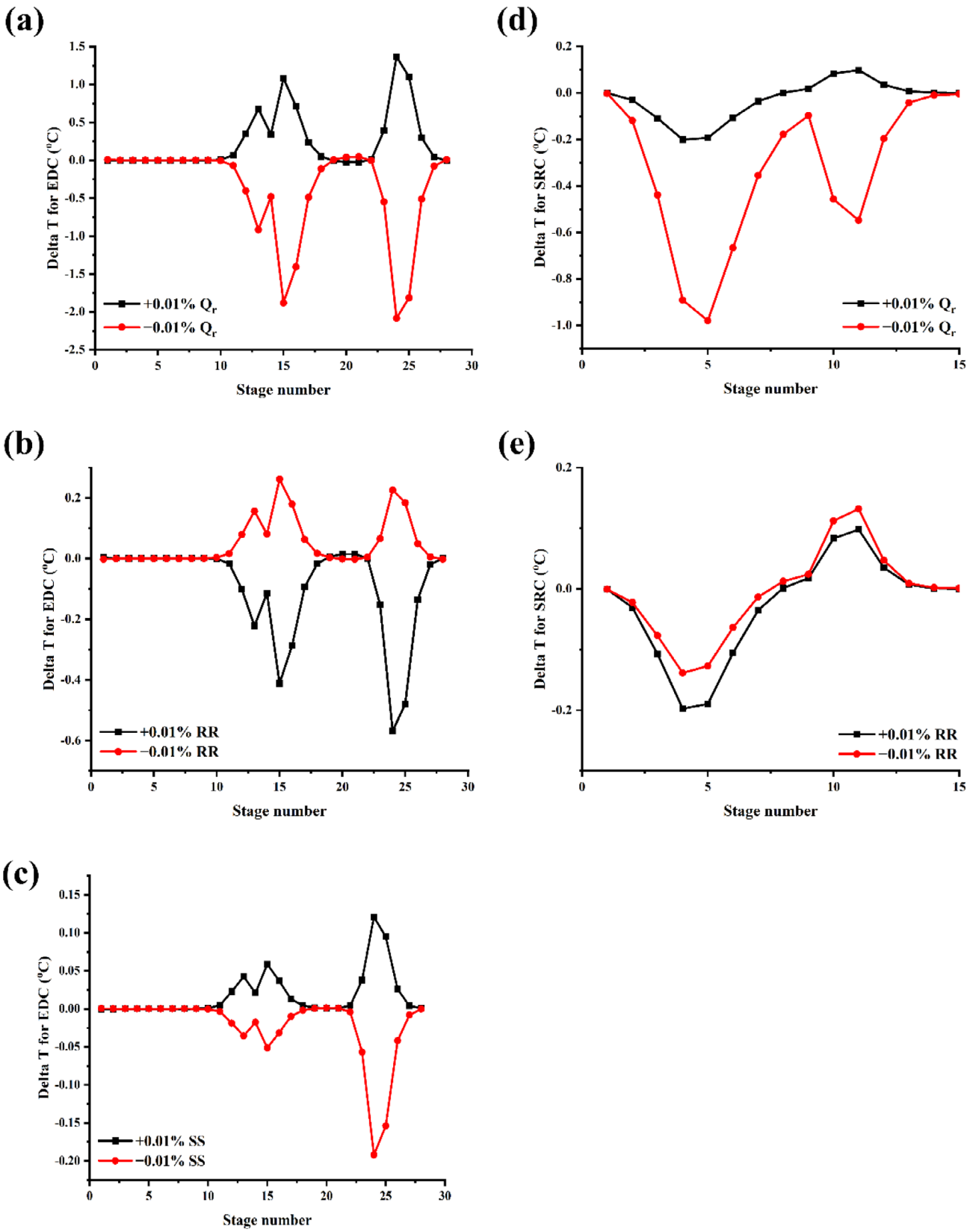

Figure 8. Sensitivity analysis for the optimized design of SSED for case 1

The control properties of both intensified processes in the present case deteriorated, as they did in the previous case and as reflected by the increase in the CN. This means that a more complex control structure is generally required. Such findings are analogous to case 1 and are consistent with existing studies, which reported that a given column configuration is strongly

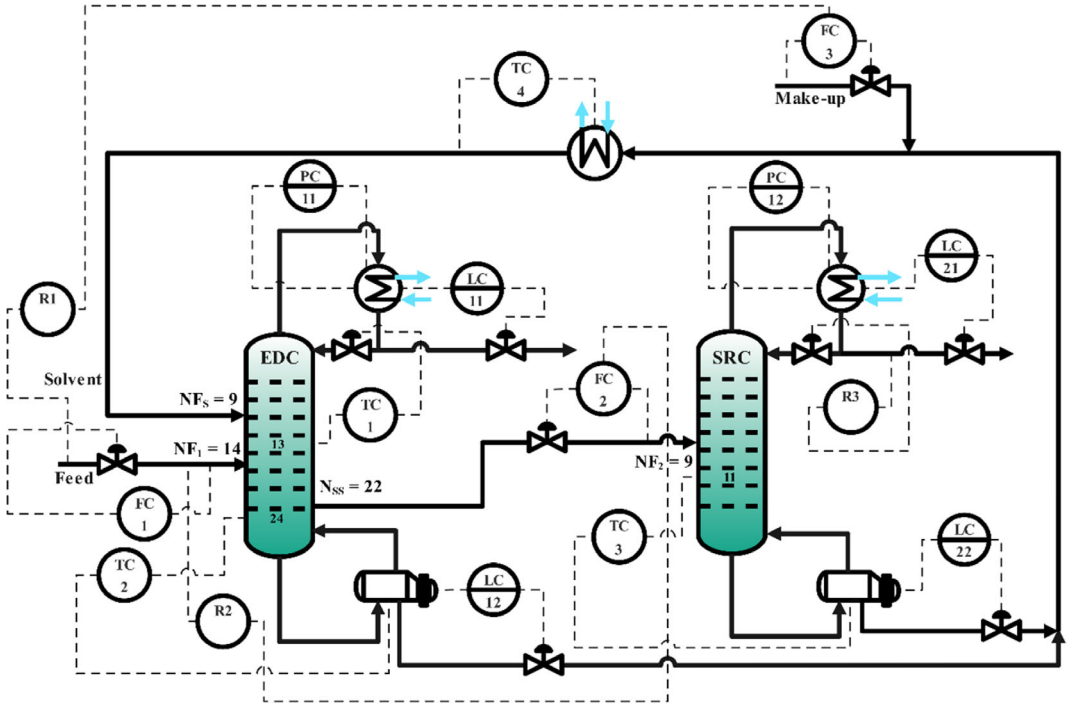

Figure 9. CS 1-1 of the optimized configuration for case 1.

associated to an exact composition mixture that affects the control properties of a process. For the preserved configuration, it was designed by preserving the original configuration from the base case, and the presence of an additional side-stream resulted in a slight change in the composition and stream flow that could impact the controllability of the process.[61] Following this, one cannot be certain that the control performance remains analogous to the base case because the configuration is no longer at its optimum point. On the other hand, the deterioration in control properties in the optimized configuration was also expected since the optimization problem was addressed based on single objective optimization and the impact of other sustainability indicators (such as control) was not considered. To this end, one can only expect the optimum design to be at the best economical

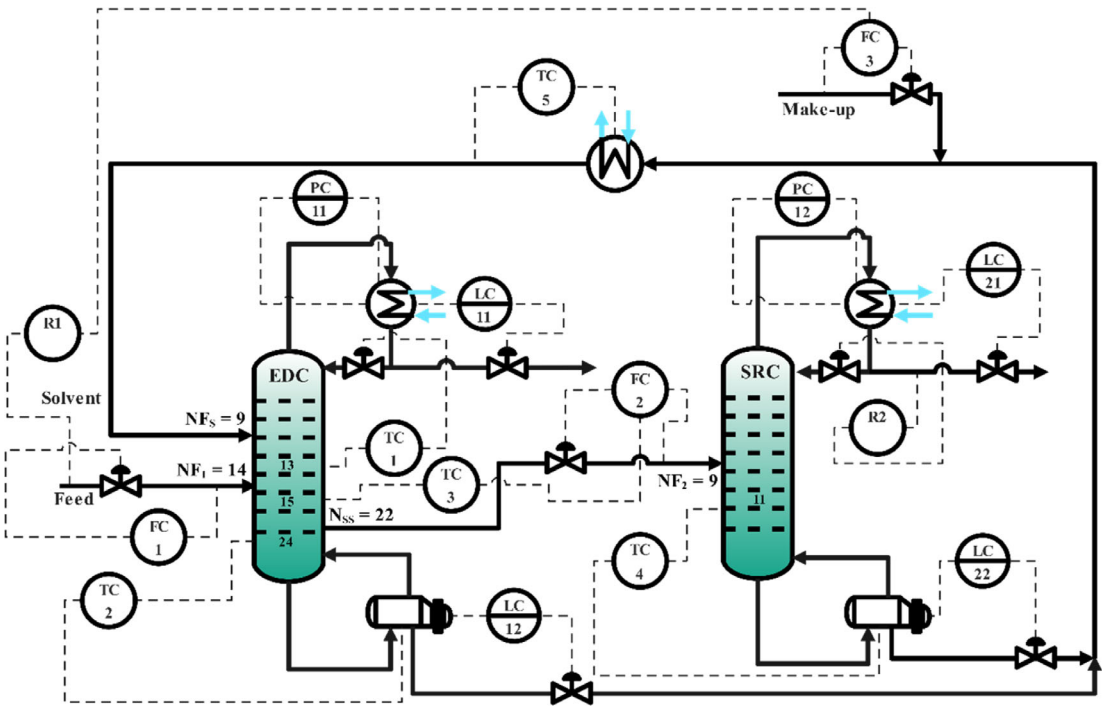

Figure 10. CS 1-2 of the optimized configuration for case 1.

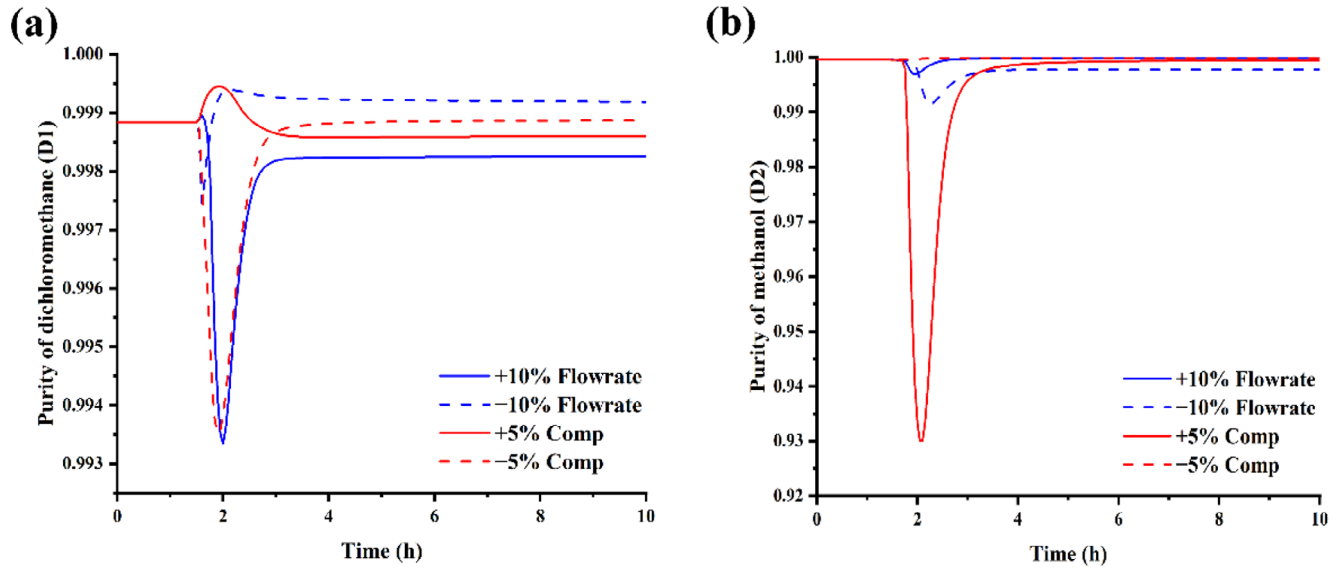

Figure 11. Dynamic responses of (a) dichloromethane and (b) methanol purities using **CS 2**.

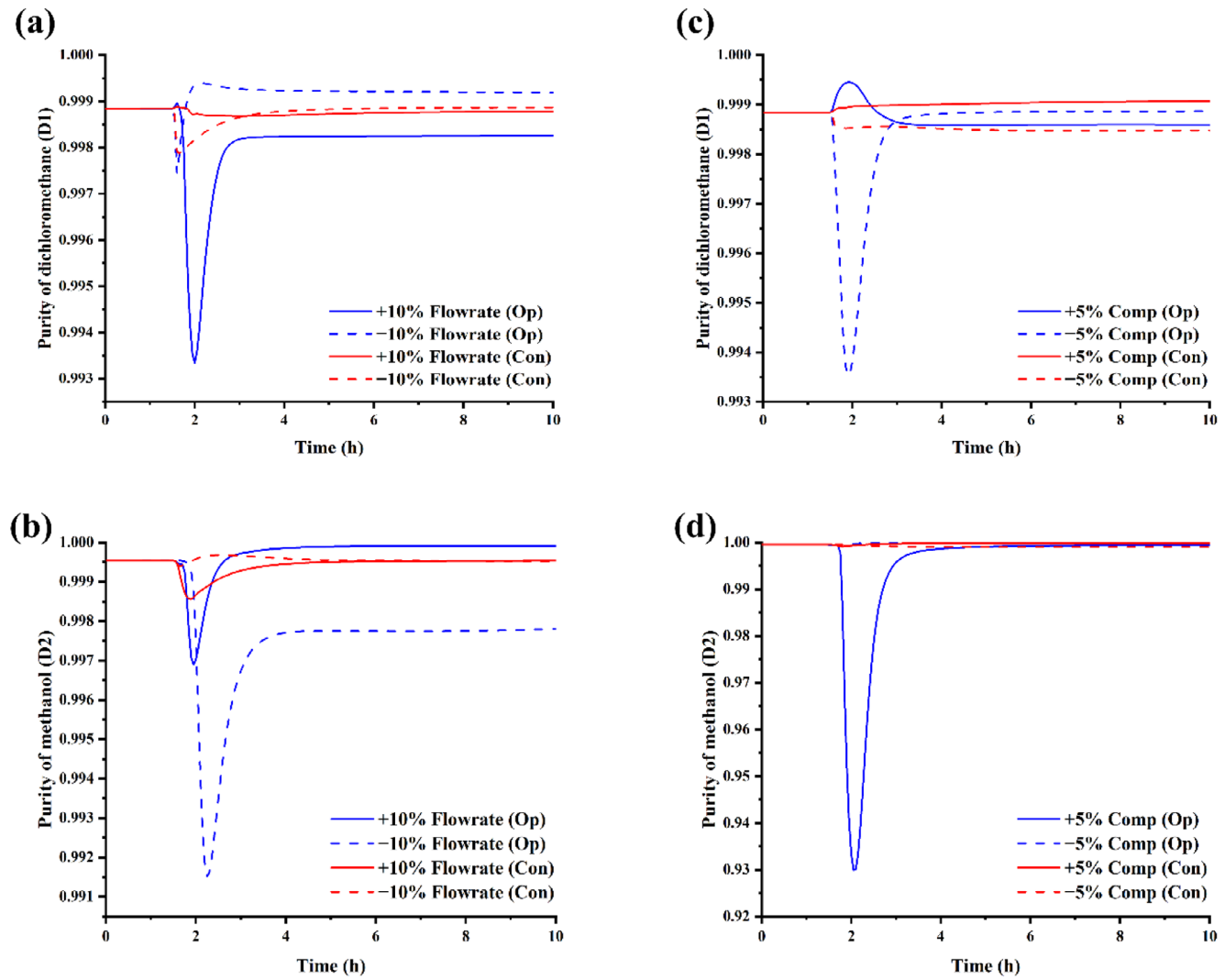

Figure 12. Dynamic response comparison between preserved (Con) and optimized configuration (Op) in terms of product purities.

point (i.e., lowest TAC), while it may not necessarily provide the best operational controllability. Here, we wish to reiterate that the previous studies[2,62,63] showing that optimization generally improves the operational controllability of a process are the same studies that involved bi-objective optimization simultaneously considering economical and theoretical control properties. Nonetheless, such multi-objective optimization is not considered in this work because the objective of this work was to preliminarily analyze the effects of designing an intensified process either by maintaining the original system design or by a complete process optimization on the different sustainability indicators. We first identified which sustainability indicators played a greater role so that these indicators can be considered for multi-objective optimization in future work.

Unlike i case 1, it appears that only the optimized process (Fig. 6(b)) provided significant improvements to most of the green metrics relative to the CED (Fig. 2). In contrast, the preserved configuration (Fig. 6(a)) only provided a reasonable enhancement to the IR and this benefit was traded-off by the increase in other green indices, such as energy, economic, environmental, and control.

Control performance

Case study 1

As indicated in the Methodology section, the SSED designed by preserving the original column configuration was reproduced directly from our previous work,[16] while only the optimized configuration was developed in this work. Thus, the control strategy of the preserved configuration is not repeated, and only the control strategy for the optimized configuration is elaborated here. Figure 8 shows sensitivity analysis result of the optimized configuration for case 1. The EDC has three control degrees of freedom, i.e., reboiler duty, reflux ratio, and side-stream flowrate (Fig. 8(a)–(c)), while two control degree of freedoms are available for the SRC column, i.e., reboiler duty and reflux ratio (Fig. 8(d), (e)). From Fig. 8, it was found that stages 13, 15, and 24 in the EDC are sensitive to changes in reboiler duty, reflux ratio, and side-stream flowrate, albeit to slightly different extents. On the other hand, only stage 11 is sensitive to the reboiler duty in the SRC.

We started off our dynamic investigation by developing a dual temperature control structure on the EDC and a single temperature control on SRC since the SRC only contains one temperature sensitive location (i.e., stage 11). In the EDC, we attempted to use the reflux ratio to maintain the temperature of stage 13 because it is the nearest to the top of the column. For the same reason, the reboiler duty was used to maintain the temperature of stage 24. The reflux ratio of SRC was fixed at its steady-state value, which is a common method in existing studies.[64,65] The resulting control structure was termed **CS 1-1** and its control structure is depicted in Fig. 9.

For the sake of a fair comparison, the robustness of **CS 1-1** for the optimized configuration was tested using identical disturbances as the preserved configuration from previous work, i.e., ±10% throughput and ± 5% feed composition disturbances; the control performances are given in Supporting Information, Figs. S1 and S2. During the throughput disturbance (Supporting Information, Fig. S1), both product purities returned to their setpoints in under 5 h. On the other hand, the purity dichloromethane dropped to about 96 mol% when the system was subjected to −5% feed composition disturbance. This is expected due to the increase in the methanol composition in the fresh feed stream, which is an impurity in the EDC. Likewise, the purity of methanol dropped drastically to an unacceptable limit of 77.5 mol% when the system was subjected to +5% feed composition disturbance. This was due to the decrease in the methanol composition in the fresh feed stream. During the feed composition disturbance, it was also observed that the temperature of stage 15 fluctuated severely and this affected the composition of the side-draw in stage 15, which subsequently affected the methanol purity in the distillate of the SRC. This is attributed to the absence of a temperature control to maintain the temperature of stage 15 (i.e., one of the temperature-sensitive stages, as evident by the sensitivity analysis in Fig. 8). Then, Supporting Information, Fig. S2 shows that all the temperature sensitive locations in both EDC and SRC were held tightly at their setpoint, except for the temperature of stage 13 in the EDC during the −5% feed composition disturbance. To further tighten the products purities, a triple point control was investigated next.

The second control structure (**CS 1-2**) (Fig. 10) relied on the triple point control concept, where the three control variables (i.e., stage 13, stage 15, and stage 24) are controlled by using three manipulating variables (i.e., reflux ratio, side-stream flowrate, and reboiler duty, respectively). The control responses of **CS 1-2** under the same disturbances are available in Figs. 11 and S3. Identical to the **CS 1-1** demonstrated earlier, **CS 1-2** enables both product purities to return to values quite close to their setpoints under throughput disturbances (Fig. 11). For the feed composition disturbance, significant improvement was observed where **CS 2** enabled both product purities to hold closely at their setpoint values under 4 h (Fig. 11), contrary to when the process is controlled using **CS 1** (Supporting Information, Fig. S1). All the temperatures in both EDC and SRC are also held tightly at their setpoint value (Supporting Information, Fig. S3). Here, it appears that the presence of an additional temperature controller enabled the product purity and the temperature of the temperature-sensitive location to return to their nominal values quickly.

When comparing the dynamic responses of both **CS 1-1** and **CS 1-2**, it becomes apparent that the **CS 1-2** provides better control performance for the optimized configuration since it can withhold both product purities and all the temperatures closely at their setpoint. Thus, **CS 1-2** was used as a benchmark for subsequent comparisons against the preserved configuration from the previous work (Supporting Information, Fig. S4). Figure 12 shows the results comparison. When comparing the control performance of the optimized configuration against that of the preserved configuration, it appears that the preserved configuration design from the previous work (Supporting Information, Fig. S4) provides better controllability in returning both product purities to a value close to their setpoint under both throughput and feed composition disturbances. In addition, the transient deviation of the preserved configuration design is also smaller in comparison to the optimized configuration. These findings are consistent with the theoretical control performance in the Case Study 1 section, where the CN was 21% smaller than that of the optimized configuration. Collectively, the dynamic superiority of the preserved configuration is clearly demonstrated with respect to the optimized configuration.

Here, the main highlight of the control performance comparison is that the temperature-sensitive locations in the EDC increase from two stages in the preserved configuration to three stages in the optimized configuration. This means that optimizing the SSED in the present scenario deteriorates the control performance of the process. The increase in the temperature-sensitive locations further results in an additional temperature controller being required to control the side-stream flowrate, without which both

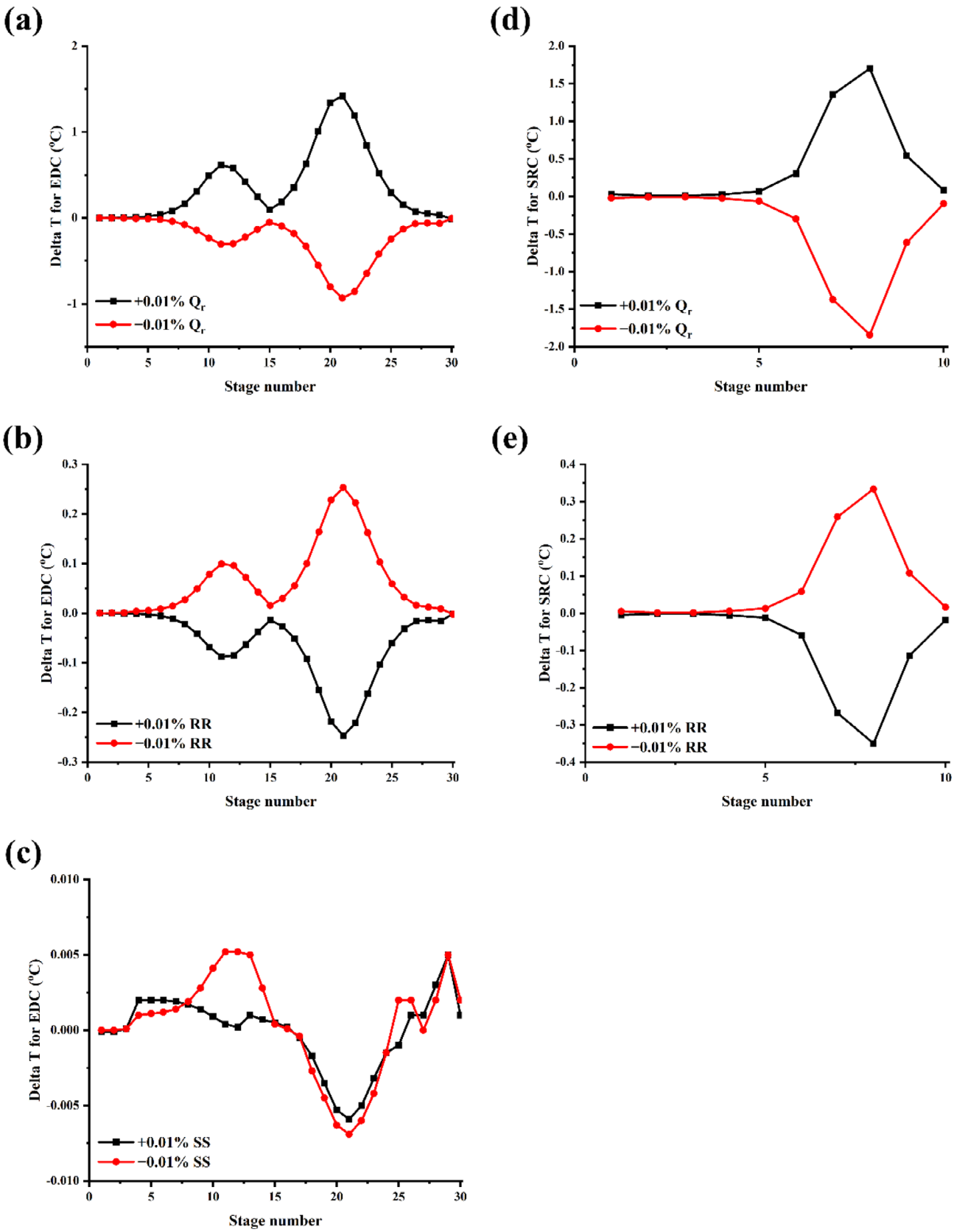

Figure 13. Sensitivity analysis for optimized configuration for case 2.

product purities will deviate to an unacceptable limit during feed composition disturbance (Supporting Information, Fig. S2). On the other hand, the temperature-sensitive locations in the SRC decreased from two stages in the preserved configuration to only one stage in the optimized configuration, signifying that a simpler control structure is required by the SRC. For the SRC, a dual

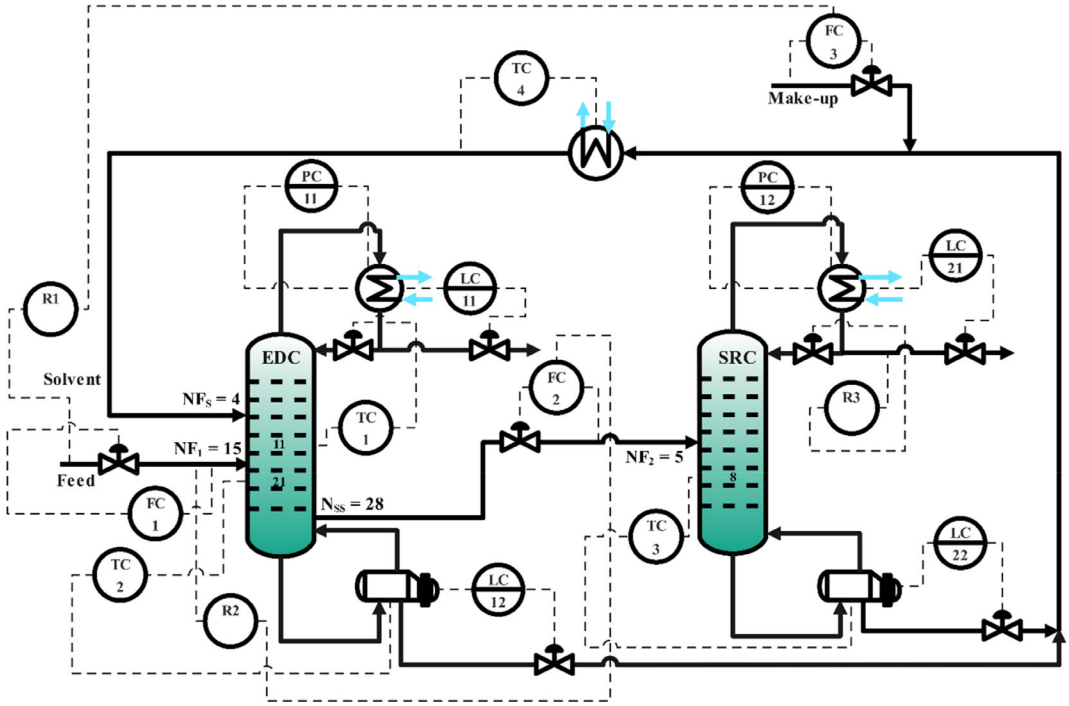

Figure 14. CS 2-2 of the optimized configuration for case 2.

temperature control is required for the preserved configuration, while the optimized configuration in this work only requires a single point temperature control. One common observation in the control performances of the preserved and optimized configuration is the relatively high transient deviation when the system is subjected to various disturbances. If such a deviation is unacceptable, a feedforward control structure must be considered (not shown in this study).

Case study 2

Unlike case 1, the control structures for both the preserved and optimized configurations were developed in this work since they have not been reported in any of the previous studies. Fig. S5 in the supporting information displays the sensitivity analysis results of the preserved configuration. Here, it appears that the EDC has two different temperature-sensitive regions that are identical to those in the preserved configuration in case 1. On the other hand, the SRC only has one temperature-sensitive region. From Supporting Information, Fig. S5, it appears that stages 10 and 18 in the EDC are strongly impacted by the changes in all three manipulating variables (e.g., reboiler duty, reflux ratio, and side-stream flowrate), making the control pairing challenging. In SRC, only stage 4 is strongly impacted by the change in reboiler duty. To this end, we attempted to develop a dual temperature control structure on the EDC and a single temperature control on SRC using reboiler duty.

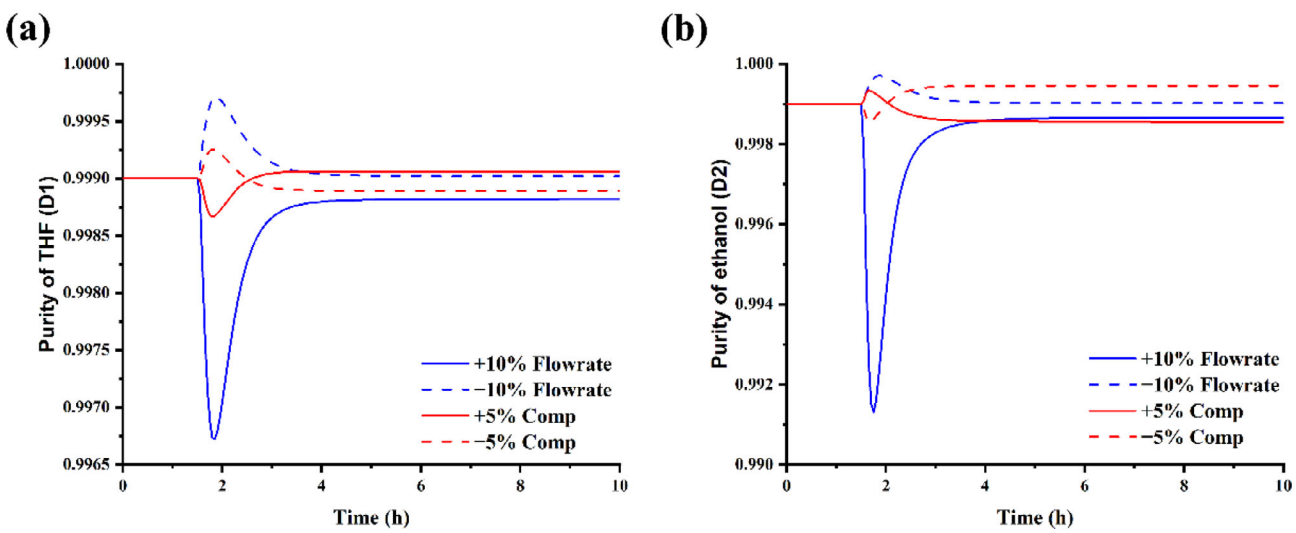

Figure 15. Dynamic responses of (a) THF and (b) ethanol for optimized configuration using **CS 2-2**.

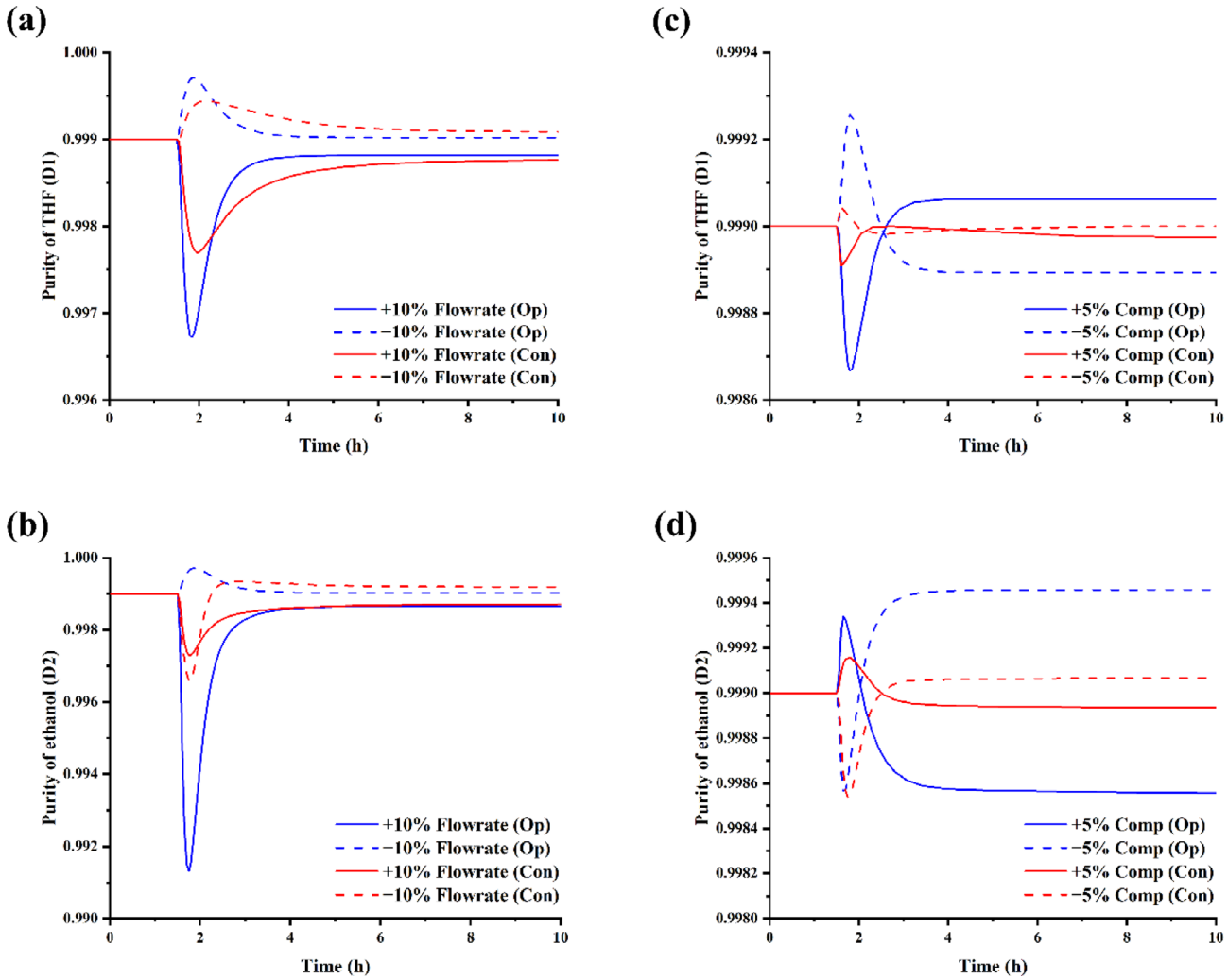

Figure 16. Dynamic response comparison between preserved (Con) and optimized configuration (Op) in terms of products purities for case 2.

In the EDC, our RGA analysis results suggests controlling stage 10 by using reflux ratio and stage 18 by manipulating the reboiler duty. The side-stream flowrate is maintained by ratio to the feed flowrate to ensure material balance. The reflux ratio of SRC is fixed at its steady-state value, identical to case 1. The resultant control structure was termed **CS 2-1** and its control structure is depicted in Supporting Information, Fig. S6.

We tested the performance of **CS 2-1** using the same disturbances used for case 1 (i.e., ±10% throughput and ± 5% feed composition disturbances) and the control performances are given in Supporting Information, Figs. S7 and S8. During the throughput and feed composition disturbances, both product purities returned to values very close to their setpoints in less than 5 h (Supporting Information, Fig. S7). All the temperature sensitive locations in both EDC and SRC were held tightly and returned to their setpoints under 5 h (Supporting Information, Fig. S8), except for the temperature of tray 10 in the EDC, which took an additional hour. In our opinion, this is expected because of the slightly large integral time and owing to the fact that stage 10 was located slightly further from the top of the column. Since all the product purities and temperature-sensitive trays could be held tightly at a values very close to their setpoints using **CS 2-1**, we explored next the dynamic performance of the optimized configuration.

The result of the sensitivity analysis for the optimized configuration is given by Fig. 13. Here, two different temperature-sensitive regions were observed in the EDC, while only one temperature-sensitive region was available for the SRC; this is analogous to the preserved configuration. One significant difference observed between the preserved and optimized configurations is that there is no tray temperature in the EDC that is sensitive to the side-stream flowrate, leaving only two manipulating variables available for control pairing in the EDC. Another difference here is that the temperature-sensitive region in the SRC is sensitive to both manipulated parameters (i.e., reflux ratio and reboiler duty).

In the EDC, our RGA results revealed that controlling stage 11 with reflux ratio and stage 21 with reboiler duty provides the best control pairing. In comparison to the preserved configuration, it appears that the temperature-sensitive locations of the column changed after process optimization (e.g., in EDC, the temperature-sensitive tray shifted from stage 18 in the preserved configuration to stage 21 in the optimized design). For the SRC, we used the reboiler duty to control the temperature of stage 8 since it is located close to the column bottom. Analogous to the preserved configuration, the side-stream flowrate in the present case was maintained by ratioed to the feed flowrate, while

the reflux ratio of SRC was fixed at its steady-state value. The resultant control structure (**CS 2-2**) is given in Fig. 14.

The control performance of the optimized configuration was tested using the same disturbances given in Figs. 15 and S9. Identical to the preserved configuration, both product purities returned to values close to their setpoints in less than 5 h (Fig. 15). Here, it is worth noting that the transient deviation for the optimized configuration is inferior in comparison to the preserved configuration. For example, during the +10% throughput disturbance, the purity of THF dropped to 99.65 mol% before returning gradually to the setpoint value. Comparatively, the purity of THF in the preserved configuration only dropped marginally to 99.77 mol%, prior to returning to its original specification. If such a deviation is intolerable, a feedforward control structure must be considered (not shown in this study). The temperatures of the temperature-sensitive locations returned to their desired setpoints quickly (i.e., in less than 5 h) (Supporting Information, Fig. S9). Here, it appears that the product purities and temperature-sensitive trays were well maintained during both throughput and feed composition disturbances, and this is identical to the results of the preserved configuration. Unlike case 1, no additional temperature control was required in the EDC because there were only two temperature-sensitive stages and the existing dual temperature controllers could effectively reject both the throughput and feed composition disturbances. We compared next the control performances of the preserved and optimized configurations for case 2, as displayed in Fig. 16.

From Fig. 16, it becomes clear that the preserved configuration provided a better control performance than the optimized configuration. This is evident from Fig. 16, where the preserved configuration provided a lower transient deviation and could return both product purities closer to their setpoints with respect to the optimized configuration. These findings align with the theoretical control performance in the Case Study 2 section, where the CN of the preserved configuration was 30% smaller than that of the optimized configuration. Relative to case 1, both the preserved and optimized configurations in case 2 only relied on the dual temperature control in the EDC, while the temperature-sensitive locations in the EDC increased from two stages in the preserved configuration to three stages in the optimized configuration in case 1. Although both intensified processes in case 2 used similar control structures, the performance of the optimized configuration was inferior compared to the preserved configuration, and this was analogous to the findings reported in case 1.

CONCLUSIONS

In this study, we compared the sustainability performance of the preserved (i.e., keeping the original column configuration) and optimized designs of an intensified SSED using two binary azeotropic separation case studies and considering economic, environmental, process safety, and process control factors. The results showed that energy savings can be achieved by preserving the original CED configuration, but optimization is necessary to guarantee it. Generally, reducing energy consumption leads to improved economics and environmental performance. The risk index for the optimized SSED was higher due to the larger column size, while the risk index for the preserved configuration showed an opposing trend. Nonetheless, the overall safety performances of the preserved and optimized SSED were similar, with only a slight difference between them, thus indicating that both designs have comparable sustainability performances. The CN for both designs increased, indicating the need for a more complex control structure. The preserved configuration had a lower CN, aligning with the control performance trend from our dynamic simulation. Overall, preserving or optimizing the SSED design each has its own benefits and drawbacks. Optimization resulted in lower TAC, energy consumption, and environmental emissions for both case studies, but at the cost of a higher risk factor and operational difficulty. Therefore, optimizing the process does not necessarily guarantee a significant enhancement in all sustainability indicators.

For future work, we recommend exploring the possibility of multi-optimizing all sustainability indicators, except for the safety index, because our analysis revealed that the economic, energy, environmental, and control indices play a more significant role in representing the sustainability of the process compared to the safety index. The safety index in this work has a negligible role in representing the sustainability of the process, as indicated by the similar performance of the preserved and optimized designs, with only a slight difference between them. Future study should also consider incorporating different weightages for the multi-objective optimization to achieve a more comprehensive and balanced sustainability performance.

ACKNOWLEDGEMENTS

Authors gratefully acknowledged the support from Sunway University Malaysia, Xiamen University Malaysia, Swinburne University of Technology Sarawak Campus, and Universidad de Guanajuato. E. Sánchez-Ramírez and J.G. Segovia-Hernández appreciate the financial support provided by CONACYT. This project was supported by the Natural Science Foundation of Chongqing, China (Grant No. CSTB2022NSCQ-MSX0655 to Ao Yang), the Science and Technology Research Program of Chongqing Municipal Education Commission (Grant No. KJQN202201516 to Ao Yang), and the Research Success Award: Publication Award 2022 (2-5800) to Jaka Sunarso. We appreciate the technical assistance given by Joo Yee Heah from the University of Science, Malaysia.

DATA AVAILABILITY STATEMENT

All data generated or analyzed during this study are available from the corresponding authors on reasonable request.

SUPPORTING INFORMATION

Supporting information may be found in the online version of this article.

REFERENCES

1 Amezquita-Ortiz JM, Alcocer-Garcia H, Contreras-Zarazua G, Fontalvo J and Segovia-Hernandez JG, Sustainable process Design for Acetone Purification Produced via dehydrogenation of 2-propanol. *Ind Eng Chem Res* **61**:3660–3671 (2022). https://doi.org/10.1021/acs.iecr.1c04321.

2 Santaella MA, Jiménez LE, Orjuela A and Segovia-Hernández JG, Design of thermally coupled reactive distillation schemes for triethyl citrate production using economic and controllability criteria. *Chem Eng J* **328**:368–381 (2017).

3 González-Navarrete C, Sánchez-Ramírez E, Ramírez-Márquez C, Hernández S, Cossío-Vargas E and Segovia-Hernández JG, Innovative reactive distillation process for the sustainable purification of lactic acid. *Ind Eng Chem Res* **61**:621–637 (2022). https://doi.org/10.1021/acs.iecr.1c04050.

4 Sánchez-Ramírez E, Hernández S, Romero-García AG, Alcocer-García H and Segovia-Hernández JG, Synthesis and optimization of sustainable processes based on liquid-liquid extraction to purify methyl ethyl ketone. *Chem Eng Process* **171**:108522 (2022).
5 Cui C, Zhang Q, Zhang X and Sun J, Eliminating the vapor split in dividing wall columns through controllable double liquid-only sidestream distillation configuration. *Sep Purif Technol* **242**:116837 (2020).
6 Cui C, Zhang X and Sun J, Design and optimization of energy-efficient liquid-only side-stream distillation configurations using a stochastic algorithm. *Chem Eng Res Des* **145**:48–52 (2019).
7 Kong ZY, Sánchez-Ramírez E, Yang A, Shen W, Segovia-Hernández JG and Sunarso J, Process intensification from conventional to advanced distillations: past, present, and future. *Chem Eng Res Des* **188**:378–392 (2022).
8 Jiménez-González C, Constable DJC and Ponder CS, Evaluating the "greenness" of chemical processes and products in the pharmaceutical industry—a green metrics primer. *Chem Soc Rev* **41**:1485–1498 (2012). https://doi.org/10.1039/C1CS15215G.
9 Kong ZY, Lee HY and Sunarso J, The evolution of process design and control for ternary azeotropic separation: recent advances in distillation and future directions. *Sep Purif Technol* **284:**120292 (2022).
10 Bravo-García J, Huerta-Rosas B, Sánchez-Ramírez E and Segovia-Hernández JG, Sustainability evaluation of intensified alternatives applied to the recovery of nylon industry effluents. *Process Saf Environ Prot* **147**:505–517 (2021).
11 Constable DJC, Curzons AD and Cunningham VL, Metrics to "green" chemistry—which are the best? *Green Chem* **4**:521–527 (2002).
12 Curzons AD, Constable DJC, Mortimer DN and Cunningham VL, So you think your process is green, how do you know?—using principles of sustainability to determine what is green – a corporate perspective. *Green Chem*:1–6 (2001).
13 Jiménez-González C and Constable DJC, *Green Chemistry and Engineering: A Practical Design Approach*. Wiley, New Jersey (2014).
14 Wu YC, Hsu PHC and Chien IL, Critical assessment of the energy-saving potential of an extractive dividing-wall column. *Ind Eng Chem Res* **52**: 5384–5399 (2013).
15 Wu YC, Lee HY, Huang HP and Chien IL, Energy-saving dividing-wall column design and control for heterogeneous azeotropic distillation systems. *Ind Eng Chem Res* **53**:1537–1552 (2014).
16 Kong ZY, Yang A, Segovia-Hernández JG, Putranto A and Sunarso J, Towards sustainable separation and recovery of dichloromethane and methanol azeotropic mixture through process design, control, and intensification. *J Chem Technol Biotechnol* **98**:213–229 (2022). https://doi.org/10.1002/jctb.7237.
17 Premkumar R and Rangaiah GP, Retrofitting conventional column systems to dividing-wall columns. *Chem Eng Res Des* **87**:47–60 (2009).
18 Zhao Y, Ma K, Bai W, Du D, Zhu Z, Wang Y *et al*., Energy-saving thermally coupled ternary extractive distillation process by combining with mixed entrainer for separating ternary mixture containing bioethanol. *Energy* **148**:296–308 (2018).
19 Yang A, Su Y, Sun S, Shen W, Bai M and Ren J, Towards sustainable separation of the ternary azeotropic mixture based on the intensified reactive-extractive distillation configurations and multi-objective particle swarm optimization. *J Clean Prod* **332**:130116 (2022).
20 Yang A, Kong ZY and Sunarso J, Design and optimisation of novel hybrid side-stream reactive-extractive distillation for recovery of isopropyl alcohol and ethyl acetate from wastewater. *Chem Eng J* **451**: 138563 (2023).
21 Yan J, Liu J, Ren J, Wu Y, Li X, Sun T *et al*., Design and multi-objective optimization of hybrid reactive-extractive distillation process for separating wastewater containing benzene and isopropanol. *Sep Purif Technol* **290**:120915 (2022).
22 Shestakova M and Sillanpää M, Removal of dichloromethane from ground and wastewater: a review. *Chemosphere* **93**:1258–1267 (2013).
23 Li X, Zhao Y, Qin B, Zhang X, Wang Y and Zhu Z, Optimization of pressure-swing batch distillation with and without heat integration for separating dichloromethane/methanol azeotrope based on minimum Total annual cost. *Ind Eng Chem Res* **56**:4104–4112 (2017). https://doi.org/10.1021/acs.iecr.7b00464.
24 Caldwell DJ, Sources of pharmaceutical residues in the environment and their control. *Issues Environ Sci Technol*:92–119 (2016). https://doi.org/10.1039/9781782622345-00092.
25 Thai PK, Ky LX, Binh VN, Nhung PH, Nhan PT, Hieu NQ *et al*., Occurrence of antibiotic residues and antibiotic-resistant bacteria in effluents of pharmaceutical manufacturers and other sources around Hanoi. *Vietnam Sci Total Environ* **645**:393–400 (2018).
26 Nassiri Koopaei N and Abdollahi M, Health risks associated with the pharmaceuticals in wastewater. *DARU J Pharm* **25**:9 (2017). https://doi.org/10.1186/s40199-017-0176-y.
27 Iqbal A, Ahmad SA and Ojasvi. Design and control of an energy-efficient alternative process for separation of dichloromethane-methanol binary azeotropic mixture. *Sep Purif Technol* **219**:137–149 (2019).
28 Luis P, Amelio A, Vreysen S, Calabro V and van der Bruggen B, Simulation and environmental evaluation of process design: distillation vs. hybrid distillation-pervaporation for methanol/tetrahydrofuran separation. *Appl Energy* **113**:565–575 (2014).
29 Wang Y, Cui P, Ma Y and Zhang Z, Extractive distillation and pressure-swing distillation for THF/ethanol separation. *J Chem Technol Biotechnol* **90**:1463–1472 (2015).
30 Yang A, Su Y, Teng L, Jin S, Zhou T and Shen W, Investigation of energy-efficient and sustainable reactive_pressure swing distillation processes to recover tetrahydrofuran and ethanol from the industrial effluent. *Sep Purif Technol* **250**:117210 (2020).
31 Su Y, Yang A, Jin S, Shen W, Cui P and Ren J, Investigation on ternary system tetrahydrofuran/ethanol/water with three azeotropes separation via the combination of reactive and extractive distillation. *J Cleaner Prod* **273**:123145 (2020).
32 Zhao Y, Zhao T, Jia H, Li X, Zhu Z and Wang Y, Optimization of the composition of mixed entrainer for economic extractive distillation process in view of the separation of tetrahydrofuran/ethanol/water ternary azeotrope. *J Chem Technol Biotechnol* **92**:2433–2444 (2017).
33 Zhao Y, Jia H, Geng X, Wen G, Zhu Z and Wang Y, Comparison of conventional extractive distillation and heat integrated extractive distillation for separating tetrahydrofuran/ethanol/water. *Chem Eng Trans* **61**:751–756 (2017).
34 Zhang X, Zhao Y, Wang H, Qin B, Zhu Z, Zhang N *et al*., Control of a ternary extractive distillation process with recycle splitting using a mixed entrainer. *Ind Eng Chem Res* **57**:339–351 (2018).
35 Zhang Q, Zeng A, Yuan X and Ma Y, Control comparison of conventional and thermally coupled ternary extractive distillation processes with recycle splitting using a mixed entrainer as separating agent. *Sep Purif Technol* **224**:70–84 (2019).
36 Yang A, Shen W, Wei S, Dong L, Li J and Gerbaud V, Design and control of pressure-swing distillation for separating ternary systems with three binary minimum azeotropes. *AIChE J* **65**:1281–1293 (2019).
37 Zhang YR, Wu TW and Chien IL, Intensified hybrid reactive-extractive distillation process for the separation of water-containing ternary mixtures. *Sep Purif Technol* **279**:119712 (2021).
38 Li J, Li R, Zhou H, Yang X, Ma Z, Sun L *et al*., Energy-saving ionic liquid-based extractive distillation configurations for separating ternary azeotropic system of tetrahydrofuran/ethanol/water. *Ind Eng Chem Res* **58**:16858–16868 (2019). https://doi.org/10.1021/acs.iecr.9b02141.
39 Tang K, Bai P, Huang C and Liu W, Separation of tetrahydrofuran-ethanol azeotropic mixture by extractive distillation. *Asian J Chem* **25**:2774–2778 (2013).
40 Wang Y, Zhang Z, Zhao Y, Liang S and Bu G, Control of extractive distillation and partially heat-integrated pressure-swing distillation for separating azeotropic mixture of ethanol and tetrahydrofuran. *Ind Eng Chem Res* **54**:8533–8545 (2015). https://doi.org/10.1021/acs.iecr.5b01642.
41 Kong ZY, Yang A, Saptoro A and Sunarso J, Revisiting the binary azeotropic separation containing tetrahydrofuran and ethanol: design and control of extractive distillation using dimethyl sulfoxide as alternative solvent. *Digital Chem Eng* **5**:100060 (2022).
42 Srinivas M and Rangaiah GP, Differential evolution with Tabu list for solving nonlinear and mixed-integer nonlinear programming problems. *Ind Eng Chem Res* **46**:7126–7135 (2007). https://doi.org/10.1021/ie070007q.
43 Vázquez-Castillo JA, Contreras-Zarazúa G, Segovia-Hernández JG and Kiss AA, Optimally designed reactive distillation processes for eco-efficient production of ethyl levulinate. *J. Chem. Technol. Biotechnol* **94**:2131–2140 (2019). https://doi.org/10.1002/jctb.6033.
44 Alcocer-García H, Segovia-Hernández JG, Prado-Rubio OA, Sánchez-Ramírez E and Quiroz-Ramírez JJ, Multi-objective optimization of intensified processes for the purification of levulinic acid involving economic and environmental objectives. *Chem Eng Process* **136**: 123–137 (2019).

45 Ibarra-Gonzalez P, Rong BG, Segovia-Hernández JG and Sánchez-Ramírez E, Multi-objective optimization methodology for process synthesis and intensification: gasification-based biomass conversion into transportation fuels. *Chem Eng Process* **162**:108327 (2021).

46 Chen YY, Kong ZY, Yang A, Lee HY and Sunarso J, Design and control of an energy intensified side-stream extractive distillation for binary azeotropic separation of n-hexane and ethyl acetate. *Sep Purif Technol* **294**:121176 (2022).

47 Li Y, Jiang Y and Xu C, Robust control of partially heat-integrated pressure-swing distillation for separating binary maximum-boiling azeotropes. *Ind Eng Chem Res* **58**:2296–2309 (2019).

48 Yang A, Shi T, Sun S, Wei S, Shen W and Ren J, Dynamic controllability investigation of an energy-saving double side-stream ternary extractive distillation process. *Sep Purif Technol* **15**:41–53 (2019).

49 Zhang Q, Hou W, Ma Y, Yuan X and Zeng A, Dynamic control analysis of eco-efficient double side-stream ternary extractive distillation process. *Comput Chem Eng* **147**:107232 (2021).

50 Luyben WL, *Distillation Design and Control Using Aspen Simulation*. John Wiley & Sons, Inc, New Jersey (2013).

51 Turton R, Bailie RC, Whiting WB and Shaeiwitz JA, *Analysis, Synthesis and Design of Chemical Processes*. Pearson Education, United Kingdom (2008).

52 Bildea CS, Győrgy R, Sánchez-Ramírez E, Quiroz-Ramírez JJ, Segovia-Hernandez JG and Kiss AA, Optimal design and plantwide control of novel processes for di-n-pentyl ether production. *J Chem Technol Biotechnol* **90**:992–1001 (2015). https://doi.org/10.1002/jctb.4683.

53 CCPS—Center for Chemical Process Safety, CCPS. Guidelines for chemical process quantitative risk analysis. *Am Inst Chem Eng* **9**:231–235 (1990).

54 Goedkoop R and Spriensma M, *Eco-Indicator 99 Manual for Designers*. PRe Consult, (2000).

55 Sánchez-Ramírez E, Segovia-Hernandez JG, Lund NL, Pinto T, Udugama IA, Junicke H *et al*., Sustainable purification of butanol from a class of a mixture produced by reduction of volatile fatty acids. *Ind Eng Chem Res.* **60**:4975–4986 (2021).

56 Klema V and Laub A, The singular value decomposition: its computation and some applications. *IEEE Trans Autom Control* **25**:164–176 (1980).

57 Luyben ML and Floudas CA, Analyzing the interaction of design and control—1. A multiobjective framework and application to binary distillation synthesis. *Comput Chem Eng* **18**:933–969 (1994).

58 Ramírez-Márquez C, Arreola-Nájera LG and Segovia-Hernández JG, Condition number as a quantitative measure of flexibility in a process. *Comput-Aided Chem Eng* **50**:1149–1154 (2021).

59 Sun S, Chun W, Yang A, Shen W, Cui P and Ren J, The separation of ternary azeotropic mixture: thermodynamic insight and improved multi-objective optimization. *Energy* **206**:118117 (2020).

60 Liu J, Yan J, Liu W, Kong J, Wu Y, Li X *et al*., Design and multi-objective optimization of reactive-extractive dividing wall column with organic Rankine cycles considering safety. *Sep Purif Technol* **287**: 120512 (2022).

61 Kong ZY, Zarazúa GC, Lee HY, Chua J, Segovia-Hernández JG and Sunarso J, Design of novel side-stream hybrid reactive-extractive distillation for sustainable ternary separation of THF/ethanol/water using mixed entrainer. *Process Saf Environ Prot* **166**:574–588 (2022).

62 Vázquez-Castillo JA, Segovia-Hernández JG and Ponce-Ortega JM, Multiobjective optimization approach for integrating design and control in multicomponent distillation sequences. *Ind Eng Chem Res* **54**:12320–12330 (2015). https://doi.org/10.1021/acs.iecr.5b01611.

63 Cabrera-Ruiz J, Santaella MA, Alcántara-Ávila JR, Segovia-Hernández JG and Hernández S, Open-loop based controllability criterion applied to stochastic global optimization for intensified distillation sequences. *Chem Eng Res Des* **123**:165–179 (2017).

64 Yang A, Chun W, Sun S, Shi T, Ren J and Shen W, Dynamic study in enhancing the controllability of an energy-efficient double side-stream ternary extractive distillation of acetonitrile/methanol/benzene with three azeotropes. *Sep Purif Technol* **242**:116830 (2020).

65 Pan Q, Shang X, Ma S, Li J, Song Y, Sun M *et al*., Control comparison of extractive distillation configurations for separating ethyl acetate-ethanol-water ternary mixture using ionic liquids as entrainer. *Sep Purif Technol* **236**:116290 (2020).

